European Journal of Neuroscience, Vol. 15, pp. 176–196, 2002

Substance P in the descending cholinergic projection to REM sleep-induction regions of the rat pontine reticular formation: anatomical and electrophysiological analyses

Kristi A. Kohlmeier,[1*] Joan Burns,[2] Peter B. Reiner[1†] and Kazue Semba[2]
[1]Kinsmen Laboratory of Neurological Research, Department of Psychiatry, School of Medicine, University of British Columbia, Vancouver, B.C., V6T 1Z3 Canada
[2]Department of Anatomy and Neurobiology, Faculty of Medicine, Dalhousie University, Halifax, Nova Scotia, B3H 4H7 Canada

Keywords: immunohistochemistry, mesopontine tegmentum, tract tracing, whole-cell patch-clamp recording

Abstract

Release of acetylcholine within the pontine reticular formation (PRF) from the axon terminals of mesopontine cholinergic neurons has long been hypothesized to play an important role in rapid eye movement (REM) sleep generation. As some of these cholinergic neurons are known to contain substance P (SP), we used anatomical, electrophysiological and pharmacological techniques to characterize this projection in the rat. Double immunofluorescence demonstrated that 16% of all cholinergic neurons within the mesopontine tegmentum contained SP; this percentage increased to 27% in its caudal regions. When double immunofluorescence was combined with retrograde tracing techniques, it was observed that up to 11% of all SP-containing cholinergic neurons project to the PRF. Whole-cell patch-clamp recordings from *in vitro* brainstem slices revealed that SP administration depolarized or evoked an inward current in a dose-dependent manner in all PRF neurons examined, and that these effects were antagonized by a SP antagonist. The amplitude of the SP-induced inward current varied with changes in the Na^+ concentration, did not reverse at the calculated K^+ or Cl^- equilibrium potentials, and was not attenuated in the presence of tetrodotoxin, low Ca^{2+} concentration or caesium ions. These data suggest that activation of a tetrodotoxin-insensitive cation channel(s) permeable to Na^+ is responsible for a SP-induced inward current at resting membrane potentials. The depolarizing actions of SP appeared to be primarily due to activation of the adenylate cyclase pathway, and were additive with cholinergic receptor activation even at maximal concentrations. These data indicate that SP is colocalized in a subpopulation of mesopontine tegmental cholinergic neurons projecting to REM sleep-induction regions of the PRF, and that actions of these two neuroactive substances on PRF neurons are additive. If SP is coreleased with acetylcholine, the additive actions of the two neurotransmitters might heighten the excitability of postsynaptic PRF neurons and ensure the initiation and maintenance of REM sleep.

Introduction

Cholinergic neurons in the mesopontine tegmentum, specifically in the laterodorsal (LDT) and pedunculopontine tegmental (PPT) nuclei, are believed to play a major role in the generation of rapid eye movement (REM) sleep. They provide the main cholinergic input to so-called REM sleep-induction regions, i.e. regions within the pontine reticular formation (PRF) in which microinjections of cholinergic agents are effective in inducing a REM sleep-like state in both cat (Baghdoyan *et al*., 1984; Vanni-Mercier *et al*., 1989; Yamamoto *et al*., 1990; Reinoso-Suárez *et al*., 1994; Garzon *et al*., 1998) and rat (Gnadt & Pegram, 1986; Bourgin *et al*., 1995; Deurveilher *et al*., 1997). However, there is evidence that endogenous peptidergic input to the PRF may also be involved in REM sleep generation (Morales *et al*., 1998) and peptides have been shown to have actions within this region of the PRF (Drucker-Colín *et al*., 1984; Bourgin *et al*., 1997; Ahnaou *et al*., 1999; Kohlmeier & Reiner, 1999; Ahnaou *et al*. 2000). Indeed, peptidergic neurons are present in the mesopontine tegmentum, and several neuropeptides have been demonstrated to be present within the cholinergic neurons (Vincent *et al*., 1983). The best known of these is substance P (SP), an undecapeptide with a wide role in neurotransmission and neuromodulation, and both SP and its mRNA are present in a subpopulation of mesopontine cholinergic neurons (Vincent *et al*., 1983; Sutin & Jacobowitz, 1990). While rostral projections of cholinergic, SP-containing mesopontine neurons have been reported (Sakanaka *et al*., 1981; Sakanaka *et al*., 1983; Vincent *et al*., 1983; Oakman *et al*., 1999), the presence of SP in the descending cholinergic pathways, including that to the PRF, has not been investigated in any detail. Substance P-immunoreactive fibres (Kungel *et al*., 1994) and SP receptor immunoreactivity (Nakaya *et al*., 1994) are present in the PRF. Substance P has been shown to have a strong excitatory action on a set of caudal pontine reticular neurons implicated in the acoustic startle response, and this effect can be potentiated by coapplication of a cholinergic agonist (Kungel *et al*., 1994). However, potential effects of this peptide on the more rostrally located, REM-induction zone neurons have not been examined previously.

Correspondence: Dr Kazue Semba, [2]Department of Anatomy and Neurobiology, as above.
E-mail: Semba@is.dal.ca

**Present address*: Department of Physiology, New York Medical College, Valhalla, NY 10595 USA.

†*Present address*: Active Pass Pharmaceuticals, Vancouver, B.C., V5Z 4H5 Canada.

Received 31 May 2001, revised 17 October 2001, accepted 8 November 2001

Because SP is colocalized in neurons known to be important for behavioural state control, we first sought to examine anatomically whether SP is present in the mesopontine cholinergic neurons that project to the PRF. We distinguished between the ventral and dorsal regions of the PRF because recent studies reported regional differences in the effectiveness of carbachol injections in inducing REM sleep in both rat (Deurveilher *et al*., 1997) and cat (Reinoso-Suárez *et al*., 1994; Garzon *et al*., 1998). We then examined whether SP has electrophysiological actions on PRF neurons within the REM sleep-induction zone, and characterized cellular mechanisms that mediate the electrophysiological response.

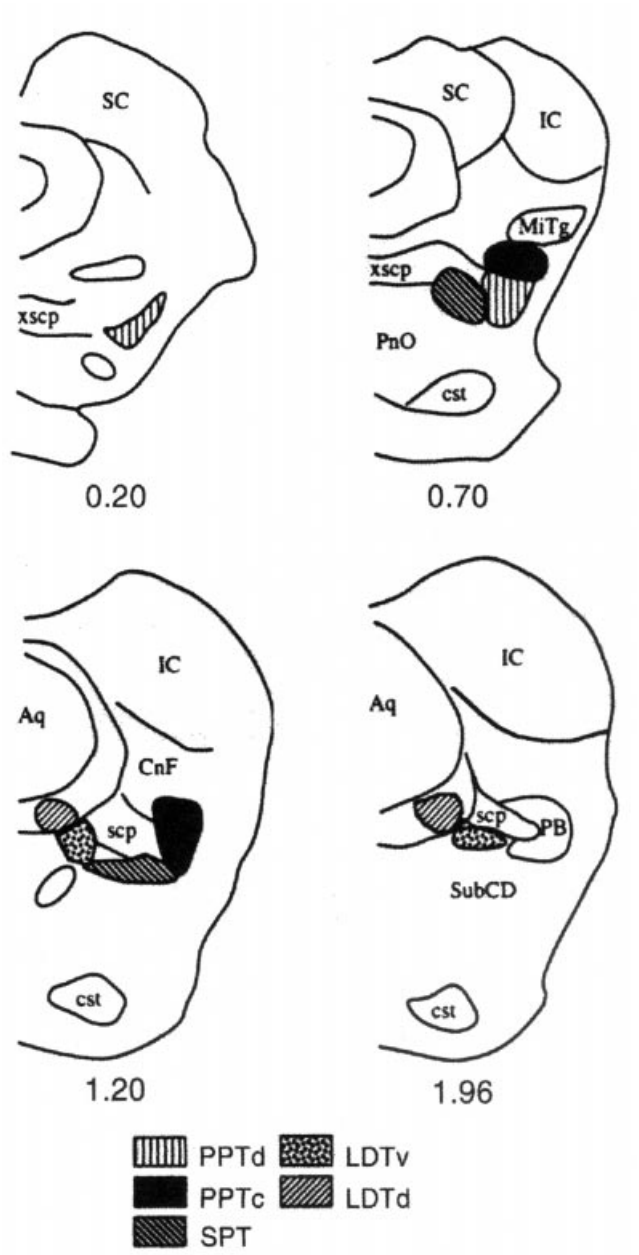

FIG. 1. Five subregions of the mesopontine tegmentum containing cholinergic neurons that were used in the quantitative analysis of single, double and triple labelled neurons. The numbers indicate estimated distances in mm from the rostral end of the column of cholinergic neurons in the mesopontine tegmentum. Modified from Inglis & Semba (1996). Abbreviations: Aq, aqueduct; cst, corticospinal tract; IC, inferior colluculus; LDTd, laterodosal tegmental nucleus (dorsal); LDTv, laterodorsal tegmental nucleus (ventral); MiTg, microcellular tegmental nucleus; PB, parabrachial nucleus; PnO, oral pontine nucleus; PPTc, pedunculopontine tegmental nucleus, pars compacta; PPTd, pedunculopontine tegmental nucleus, pars dissipata; SC, superior colliculus; scp, superior cerebellar peduncule; SPT; subpeduncular nucleus; SubCD, subcoeruleal nucleus (dorsal); xscp, decussation of the superior cerebellar peduncle.

Methods

All animals were handled in accordance with the guidelines of the Canadian Council on Animal Care, and the protocols involving animal use were approved by respective local committees at Dalhousie University and the University of British Columbia.

Anatomical studies

Animals

Twenty-one Wistar rats, 250–350 g in body weight, from Charles River Canada (St. Constant, Quebec, Canada) were used. They were kept under a 12-h light : 12-h dark cycle with lights on at 07.00 h. Food and water were available *ad libitum*.

Tracer injections

Animals were anaesthetized (i.p.) with a mixture of ketamine (10 mg/mL), xylazine (1 mg/mL) and acepromazine maleate (1 mg/mL) at 0.1 mL/100 g body weight. Using a glass micropipette attached to a Hamilton syringe, the retrograde tracer Fluorogold (FG; Fluorochrome, Englewood, CO, USA; 0.5% in saline, 5 nL) was injected into the ventral or the dorsal region of the PRF where microinjections of carbachol have been reported to be effective in inducing REM sleep in rat (Gnadt & Pegram, 1986; Bourgin *et al*., 1995; Deurveilher *et al*., 1997). The dorsal (Baghdoyan *et al*., 1984; Vanni-Mercier *et al*., 1989; Yamamoto *et al*., 1990) and ventral (Reinoso-Suárez *et al*., 1994; Garzon *et al*., 1998) PRF regions also corresponded to those reported previously in cat. The following co-ordinates were used, according to the brain atlas by Paxinos & Watson (1998): 8.5 mm posterior to bregma, 1.0 mm from midline, 8.0 mm from dura for the ventral PRF; 8.5 mm posterior to bregma, 1.0 mm from midline, 6.9 mm from dura for the dorsal PRF. After 48 h, to allow transport of the tracer, animals were re-anaesthetized as above, and colchicine (Sigma, Oakville, Ontario, Canada; 40 μg in 10 μL saline) was injected into the lateral ventricle. Twenty-four hours after colchicine injection, under anaesthesia as above, the animals were perfused with 50 mL of 0.1 M phosphate-buffered saline at room temperature, followed by 400 mL of 4% paraformaldehyde solution in 0.1 M phosphate buffer at 4 °C. Brains were cryoprotected in 30% sucrose in phosphate buffer.

Brains were cut on a freezing microtome at a thickness of 40 μm, and sections were collected in five sets in 0.05 M Tris-buffered saline. One set was immediately mounted on chrome alum, gel-coated glass slides and examined for placement of tracer injection and presence of retrogradely labelled neurons. The other sets were used for immunohistochemistry as follows, or stored as 'back-ups'.

Immunohistochemistry

One series (from a total of five series) of free-floating serial sections through the mesopontine tegmentum were processed for double immunofluorescence for ChAT (monoclonal; Boehringer-Mannheim, Laval, Quebec, Canada; 1 : 50) and SP (rabbit polyclonal; Incstar,

Stillwater, MN, U.S.A.; 1 : 800). The immunohistochemical protocol used in the present study has been described previously (Semba, 1993). The location of each of the primary antibodies was detected by a secondary antibody conjugated with Texas Red (red fluorescence) or fluorescein isothiocyanate (FITC)/Cy2 (green fluorescence). The combination most commonly used in the present study was Texas Red for ChAT and FITC/Cy2 for SP, and the two were processed sequentially in this order. In addition, two sets of sections, including a second series from the same animal, were processed with the fluorochromes switched between ChAT and SP. In four animals, one series of sections was also processed only for SP or for ChAT, using secondary antibodies tagged with one of the three fluorochromes. Control sections were reacted with omission of the primary antibodies.

Anatomical data analysis and digital imaging

Fluorescent labels were examined on an Olympus microscope with filter cubes for ultraviolet, blue and green fluorescence. Exposure to fluorescence was minimized with frequent use of the shutter on the microscope and storage of slides in darkness at 4 °C.

Examinations of immunostained sections indicated that cholinergic neurons in the mesopontine tegmentum were distributed over approximately 15 consecutive sections in each of the five series. For cell counting, in each brain, equally spaced (usually every third section) six sections that encompassed the entire mesopontine tegmentum were examined on both sides of the brain. Single, double and triple labelled neurons were plotted using an X–Y plotting program (Scope Plotter, Version 1.51; Scott Pronych, Dalhousie University, Halifax, Nova Scotia, Canada) with scaling bars attached to the microscope stage. The outline of each section was also drawn. The combined drawings were imported into DeltaGraph (Version 2.02b; SPSS, Chicago, IL, U.S.A.) for total cell counts in each section, and then into Canvas (version 3.5; Deneba Systems, Miami, FL, U.S.A.) for counts of single, double and triple labelled cells.

For quantitative analysis, the area containing the cholinergic cell group in the mesopontine tegmentum was divided into five subregions as in our previous study (Inglis & Semba, 1996) with minor modifications (Fig. 1). The five subregions were: the pars dissipata (PPTd) and pars compacta (PPTc) of the pedunculopontine tegmental nucleus, the subpeduncular nucleus (SPT), and the ventral part (LDTv) and the dorsal part (LDTd) of the laterodorsal tegmental nucleus. These subregions were demarcated in each section analysed, and labelled neurons were counted within each subregion. The numbers were added for each subregion across the six sections in each animal. The counts were expressed as mean ± SEM, and were statistically analysed by using three-way ANOVA with two repeated measures and *post hoc* Bonferroni–Dunn tests (Statview, Version 5.0; SAS Institute, Cary, NC, USA).

The cell counts used in this study were not intended for absolute numbers of cells, but rather, used as measures for the proportions of different transmitter and connectional phenotypes of mesopontine cholinergic neurons. Therefore, stereological methods were not used. Selected images of triple labelled neurons were captured on a fluorescence microscope and processed using Adobe Photoshop (version 4.0; Adobe Systems, San Jose, CA, U.S.A.) for presentation.

In vitro *electrophysiological study*

Wistar rats (7–21 days old) obtained from University of British Columbia Animal Care (Vancouver, British Columbia, Canada) were anaesthetized with halothane and decapitated. The brain was rapidly removed and trimmed to form a block that contained the REM sleep-induction zone within the PRF which was then cut into coronal slices, 400 μm-thick, on an Oxford vibratome (TPI, Tustin, CA, USA). The slice containing the PRF was placed in a recording chamber and constantly superfused with a solution of standard artificial cerebrospinal fluid (ACSF) containing (in mM): NaCl, 126; $NaHCO_3$, 25; NaH_2PO_4, 1.2; KCl, 2.5; $CaCl_2$, 2.5;, $MgCl_2$, 1.2 and glucose, 11; pH 7.3 when saturated with 95% O_2/5% CO_2, and an osmolarity of 315 mOsM. Slices were allowed to equilibrate to room temperature for ~1 h, and all electrophysiological experiments were carried out at 21 °C.

The whole-cell configuration of the patch-clamp technique as applied to brain slices was used to record from neurons in the PRF using bridge mode and voltage clamp methodologies (for details, see Kamondi *et al.*, 1992). Bridge mode and single-electrode voltage-clamp (SEVC) measurements were obtained with an Axoclamp 2A amplifier (Axon Instruments, Inc., Foster City, CA, USA). Patch pipettes were constructed from thin-wall borosillicate glass capillary tubes (1.5 mm o.d.; 1.17 mm i.d.; Warner Instrument Co., Hamden, CT, USA). The electrode solution contained (in mM): K-gluconate, 120; HEPES acid, 10; NaCl, 24; KCl, 15; EGTA, 11; $CaCl_2$, 1; MgATP, 2 with the pH ranged from 7.1 to 7.3. Osmolarity of the patch solution was 290 mOsM.

For voltage command generation, and voltage and current data acquisition, the P-Clamp 6 suite of programs (Axon Instruments Inc.) was utilized. In bridge mode, baseline and postdrug recording of synaptic activity, input resistance and resting membrane potentials of PRF neurons were collected and compared; input resistance was determined by maximum voltage deflection of the membrane potential upon the injection of 0.03 nA hyperpolarizing current following injection of DC current to bring the cell to resting membrane potential. In 'additivity' experiments, peak-induced inward current was utilized as the index of response. Data are reported as mean ± SEM Statistical significance was assessed using Student's paired *t*-test or a between group repeated measure ANOVA.

Substance P was obtained from Sigma (Oakville, Ontario, Canada) and stock solutions were made by dissolving the peptide in distilled water and then freezing this solution in 10 μL aliquots. Unless noted otherwise, on the day of the experiment, the aliquot was unfrozen and diluted to a final concentration of 250 nM in ACSF. Applications of SP were via the bath (total application time 30 s). (D-Arg^1, D-Pro^2, D-$Trp^{7,9}$, Leu^{11}) Substance P, an antagonist of SP at neurokinin receptors (Peptide Institute, Inc., Louisville, KY, USA) that does not differentiate between neurokinin receptor subtypes, was dissolved in water and applied in the ACSF at a final concentration of 1 μM.

In most experiments, tetrodotoxin (TTX; Sigma) was added to block voltage dependent Na^+ currents. To block I_h channels and the inwardly rectifying K^+ channel, caesium was added to the ACSF at 1 mM concentration. The low Na^+ (27.2 mM) solution was made by equimolar substitution of choline chloride for NaCl. In these experiments, atropine (5 μM; Sigma), an antagonist of muscarinic cholinergic receptors, was added to ACSF-choline to prevent depolarization produced by choline itself. Low Ca^{2+} (0.5 mM) solutions were made by substitution of Ca^{2+} with high Mg^{2+} (10 mM). Low Ca^{2+} ACSF was applied for 10–20 min prior to test drug application in order to ensure its effect. Effectiveness of the low Ca^{2+} solution was determined in bridge mode by monitoring the afterhyperpolarization (AHP) amplitude following elicitation of an action potential; maximal effect of the low Ca^{2+} solution was considered to have occurred when the amplitude of the AHP was significantly decreased (Gerber *et al.*, 1991; Kohlmeier & Reiner, 1999). 8-bromo-cAMP and 8-bromo-cGMP (Sigma) were dissolved in ACSF and applied for 15–20 min for maximum effect. Stock solutions of 2′5 didoxyadenosine (Calbiochem, Windsor, Ontario,

Canada; 10 mM) and RP-8-pCPT-cGMPs (Biolog, LaJolla, CA, USA; 1 mM) were prepared by dissolving them in DMSO and water, respectively. Aliquots of stock solutions were dissolved in ACSF and applied 15–20 min prior to SP.

Results

Anatomical analysis

Injection sites and immunohistochemical controls

Of 21 animals injected with FG, nine cases were subjected to quantitative analysis on the basis of the location and the size of injection. Three additional cases with dorsal PRF injection were examined qualitatively. These injection sites varied somewhat in location and size, but all were confined to the PRF. Depending on the dorsoventral position within the PRF, these injections were grouped into the ventral (Fig. 2) or the dorsal PRF cases (Fig. 3). The ventral PRF injections were located ventromedial to the motor trigeminal nucleus, at the rostral level of the caudal pontine reticular nucleus, extending, in same cases, to the caudal level of the oral pontine reticular nucleus. The dorsal PRF injections were located medial or mediodorsal to the motor trigeminal nucleus. As a group, these injections were slightly more rostral to the ventral PRF injections and centred about the junction of the oral and caudal pontine reticular nuclei, although the two sets of injections overlapped considerably.

Figure 4 illustrates examples of neurons that are triple-labelled for FG, ChAT and SP (FG+ ChAT+ SP+) or double-labelled for SP and ChAT (SP+ ChAT+). Control sections that were processed with omission of primary antibodies resulted in no specific labelling. Switching the fluorochromes of secondary antibodies between Texas Red and FITC/Cy2 made no noticeable difference in the pattern or the number of triple labelled neurons when examined in two cases. In two animals, in addition to double immunofluorescence, two series of sections were processed for either ChAT or SP. The quantitative analyses of these data indicated no obvious difference between these single immunolabelling data and those from sections processed for double immunofluorescence; indicating that triple labelling procedures did not compromise the sensitivity of detection of each marker and that the microscopic equipment used in the present study was adequate for detecting three fluorescent markers independently without interaction.

Distribution of cholinergic or SP-containing neurons: single labelling for ChAT or SP

The distribution of ChAT-immunoreactive (ChAT+) neurons was in accordance with previous reports in rat (Semba & Fibiger, 1989). The numbers of ChAT+ neurons contralateral to injection site were compared across the five subregions of the mesopontine tegmentum (Fig. 1). Regional differences were statistically significant (ANOVA, $F_{4,32} = 20.19$, $P < 0.001$; Fig. 5A), with the LDTd containing a larger number of ChAT+ neurons than any other subregion (Bonferroni–Dunn test, $P < 0.001$). Thus, the LDTd contained 37% of total ChAT+ neurons in the mesopontine tegmentum. In addition, the SPT contained significantly fewer ChAT+ neurons than the PPTd ($P < 0.001$; Fig. 5A)

The distribution of SP-immunoreactive (SP+) neurons in the midbrain and pons was also consistent with previous reports in rat (Vincent *et al*., 1983; Sutin & Jacobowitz, 1990). Large SP+ neurons were mixed with large ChAT+ neurons in the mesopontine tegmentum. Substance P+ neurons were also seen in the central grey and in the superior and inferior colliculi, but these neurons were generally smaller than those in the LDT and PPT. In the present study, only SP+ neurons within the cholinergic cell nuclei of the mesopontine tegmentum were included in quantitative analysis. The numbers of SP+ neurons were significantly different among the five subregions of the mesopontine tegmentum ($F_{4,32} = 30.93$, $P < 0.001$; Fig. 5C); SP+ neurons were seldom seen in the PPTd, whereas the LDTd contained a significantly greater number of SP+ cells than any other subregion ($P < 0.001$) and this amounted to 65% of all SP+ neurons in the cholinergic mesopontine tegmentum (Fig. 5C).

Colocalization of SP in cholinergic neurons: double labelling for SP and ChAT

The ratio of SP+ cells to ChAT+ cells showed regional differences; it was approximately 1 : 2 in the LDTd, but significantly smaller in other regions (Fig. 5A and C). The mean proportion of ChAT+ neurons that were SP+ increased from 2% to 27% in a rostral to caudal direction, with an overall average of 16% (Fig. 5B). The majority (55–66%) of SP+ neurons were ChAT+ in all subregions, except in the PPTd, where the percentage was lower, at 23% (Fig. 5D).

The number of neurons that were both ChAT+ and SP+ (ChAT+ SP+) showed a significant regional difference ($F_{4,32} = 24.83$, $P < 0.001$; Fig. 5E). The majority (64%) of such double-labelled neurons were located within the LDTd, and the number of ChAT+ SP+ neurons in this region was significantly greater than in any other region ($P < 0.001$).

Cholinergic neurons projecting to the ventral and dorsal PRF: double labelling for ChAT and FG

The comparison of ChAT+ neurons that were labelled retrogradely from the ventral and the dorsal PRF indicated that twice as many ChAT+ neurons were labelled retrogradely from the ventral, than the dorsal, PRF with FG ($F_{1,7} = 13.73$, $P < 0.01$; Figs 6 and 7A and B). The interaction between the target regions (ventral/dorsal PRF) and mesopontine subregions was also significant ($F_{4,28} = 3.86$, $P < 0.01$), but *post hoc* tests failed to detect significant differences between the dorsal and ventral injections in any of the five subregions. There was no significant overall regional difference among the five subregions.

When ventral and dorsal injections were combined, there was no significant difference in the total number of retrogradely labelled ChAT+ neurons between the ipsi- and contralateral sides. However, the numbers of FG+ ChAT+ neurons tended to show ipsilateral dominance with the dorsal PRF injections, whereas the numbers were bilaterally similar with the ventral PRF injections (Figs 6 and 7A). Thus, 16% of all ChAT+ neurons either ipsi- and contralaterally were labelled from the ventral PRF, whereas following the dorsal PRF injections, the percentage was 8% ipsilaterally, and 5% contralaterally (Fig. 7B).

SP-containing neurons projecting to the PRF: double labelling for SP and FG

A subpopulation of SP+ neurons intermixed with ChAT+ neurons were labelled retrogradely from the PRF with FG. The mean percentage of FG+ neurons among all SP+ neurons ranged from 4–8% in different subregions of the mesopontine tegmentum. As the number of such neurons was relatively small, combined data for the five subregions are shown in Fig. 7C. Similar to the results with ChAT+ neurons, FG+ SP+ neurons were bilaterally distributed following ventral PRF injections, but showed an ipsilateral dominance with dorsal PRF injections (Fig. 7C and D). Consistent with this

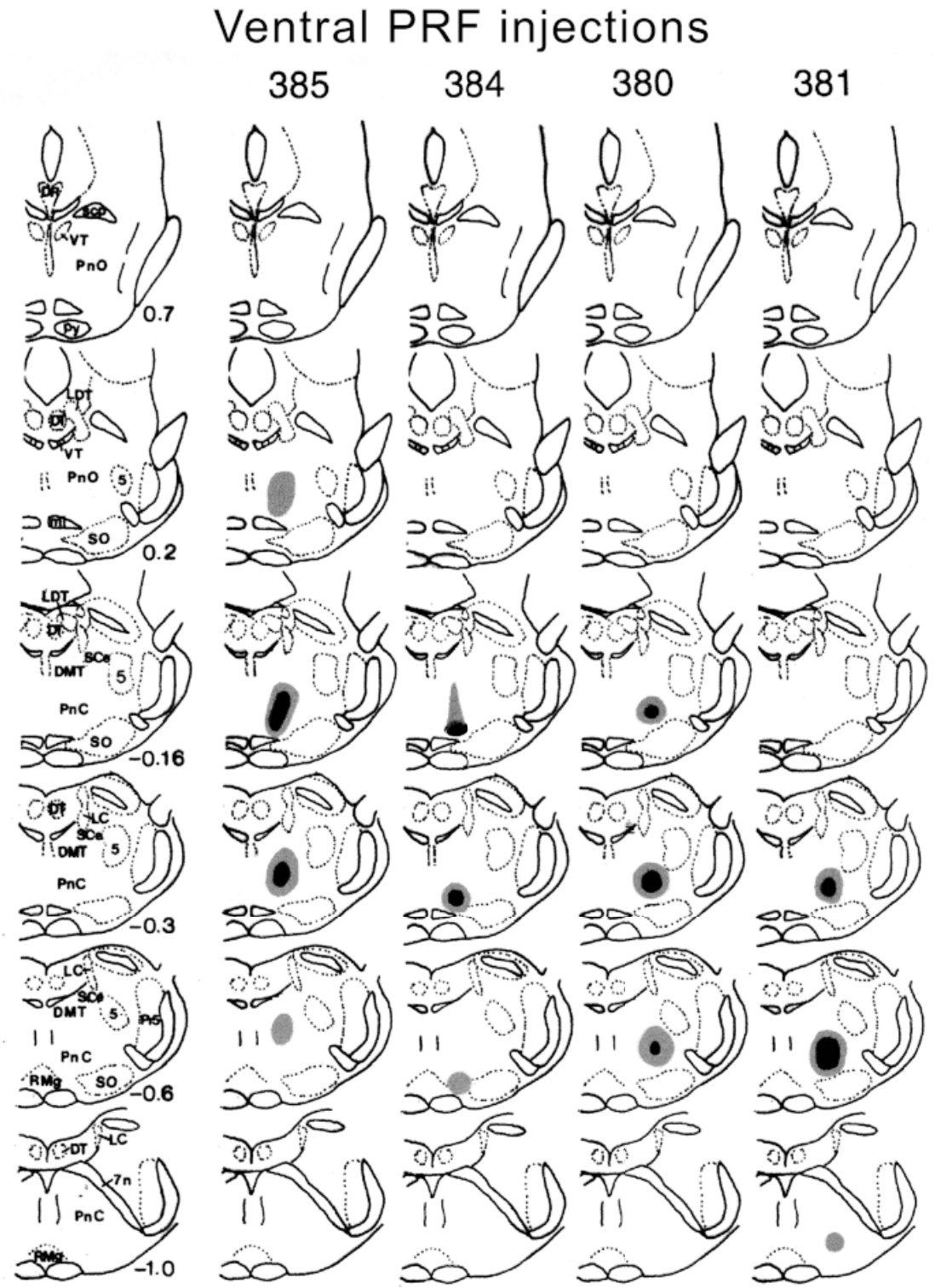

FIG. 2. Fluorogold (FG) injections into the ventral PRF in four rats. The centre of the injection is indicated with solid shading, and the halo is indicated by lighter shading. The far left column shows standardized sections at eight rostrocaudal levels of the midbrain and pons, and major structures present at each level. The number lower right to each drawing indicates the distance in mm from the interaural line according to Paxinos & Watson (1998). Abbreviations: 5, motor trigeminal nucleus; 7n, facial nerve; DMT, dorsomedial tegmental area; DR, dorsal raphe nucleus; DT, dorsal tegmental nucleus; LC, locus coeruleus; LDT, laterodorsal tegmental nucleus; ml, medial lemniscus; PnC, pontine reticular nucleus, caudalis; PnO, pontine reticular nucleus, oralis; Pr5, principal sensory trigeminal nucleus; Py, pyramidal tract; RMg, raphe magnus nucleus; SCe, subcoeruleus nucleus; scp, superior cerebellar peduncle; SO, superior olivary nucleus; VT, ventral tegmental nucleus.

trend, ANOVA revealed a significant interaction between sides and FG injection sites ($F_{1,7} = 6.12$, $P < 0.05$). Although the number of double-labelled neurons tended to be small, there was a tendency that with dorsal PRF injections, more FG+ SP+ neurons were labelled in the LDTd than in other subregions, whereas with ventral PRF injections, the LDTv had the largest number of such neurons. None of

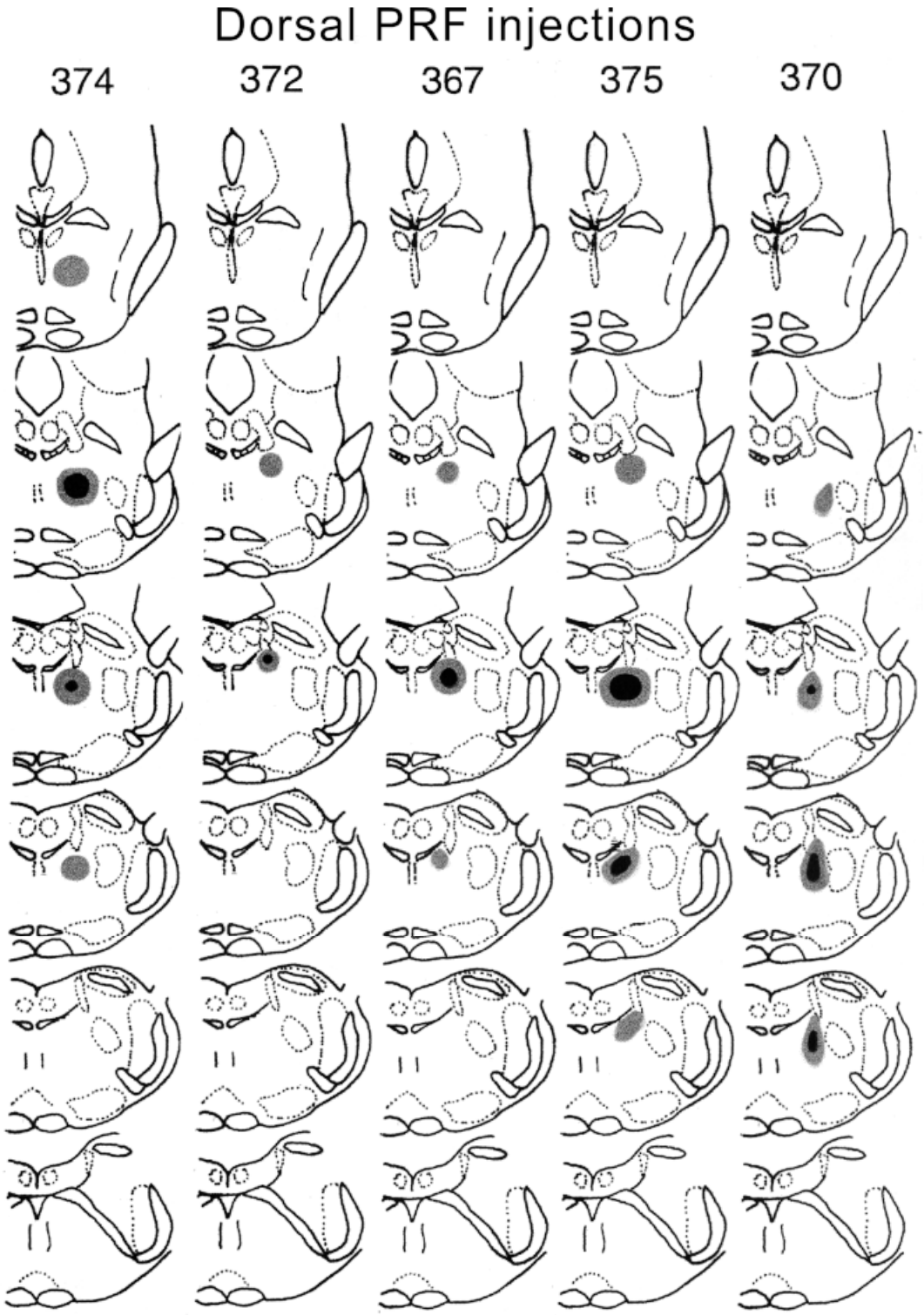

FIG. 3. Fluorogold gold injections into the dorsal PRF in five rats. The centre of the injection is indicated by solid shading, and the halo by lighter shading. See Fig. 2 for identification of structures, rostrocaudal levels, and abbreviations.

the SP+ neurons in the midbrain and pons that were outside of the cholinergic nuclei was labelled retrogradely with FG.

SP-containing cholinergic neurons projecting to the PRF: triple labelling for ChAT, SP and FG

Depending on the injection site within the PRF and the laterality, a mean percentage of 4–11% of ChAT+ SP+ neurons were labelled retrogradely from the PRF. Triple-labelled neurons were more numerous contralaterally after ventral PRF injections, whereas, there was ipsilateral dominance after dorsal PRF injections (Fig. 7E and F). Consistent with this, ANOVA indicated a significant interaction between side and injection site ($F_{1,7} = 9.48$, $P < 0.05$). Although the LDTd had the majority of ChAT+ SP+ neurons, the number of triple labelled neurons tended to be greater in the LDTv than in other

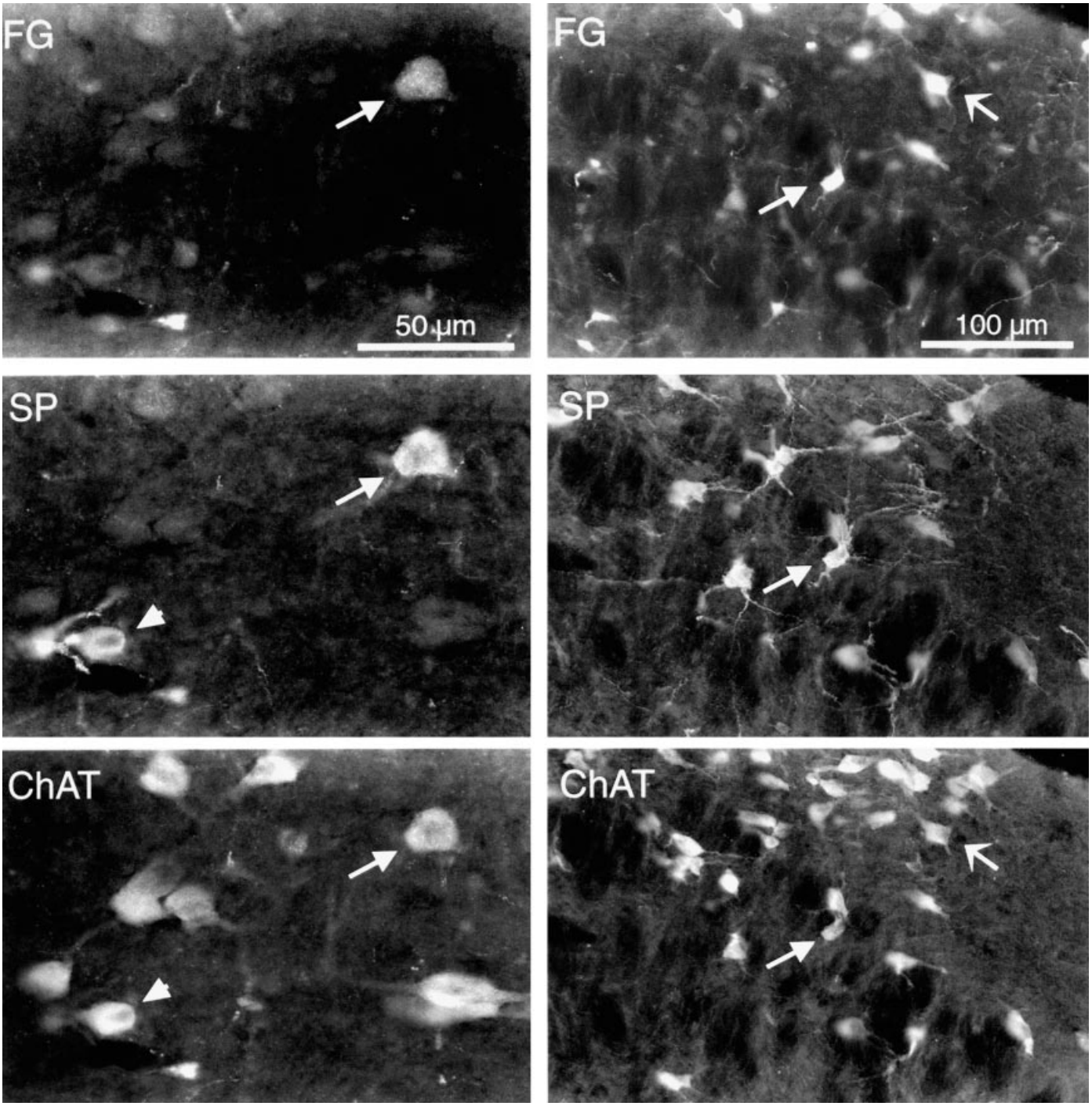

FIG. 4. Fluorescence micrographs showing two examples of triple (FG, ChAT and SP) labelled neurons (long arrows) in the LDTv (left column) and LDTd (right column), respectively. Arrowheads in the left column indicate a neuron immunoreactive for SP and ChAT, but not labelled retrogradely with FG, whereas short arrows in the right column indicate a ChAT-immunoreactive neuron labelled retrogradely with FG

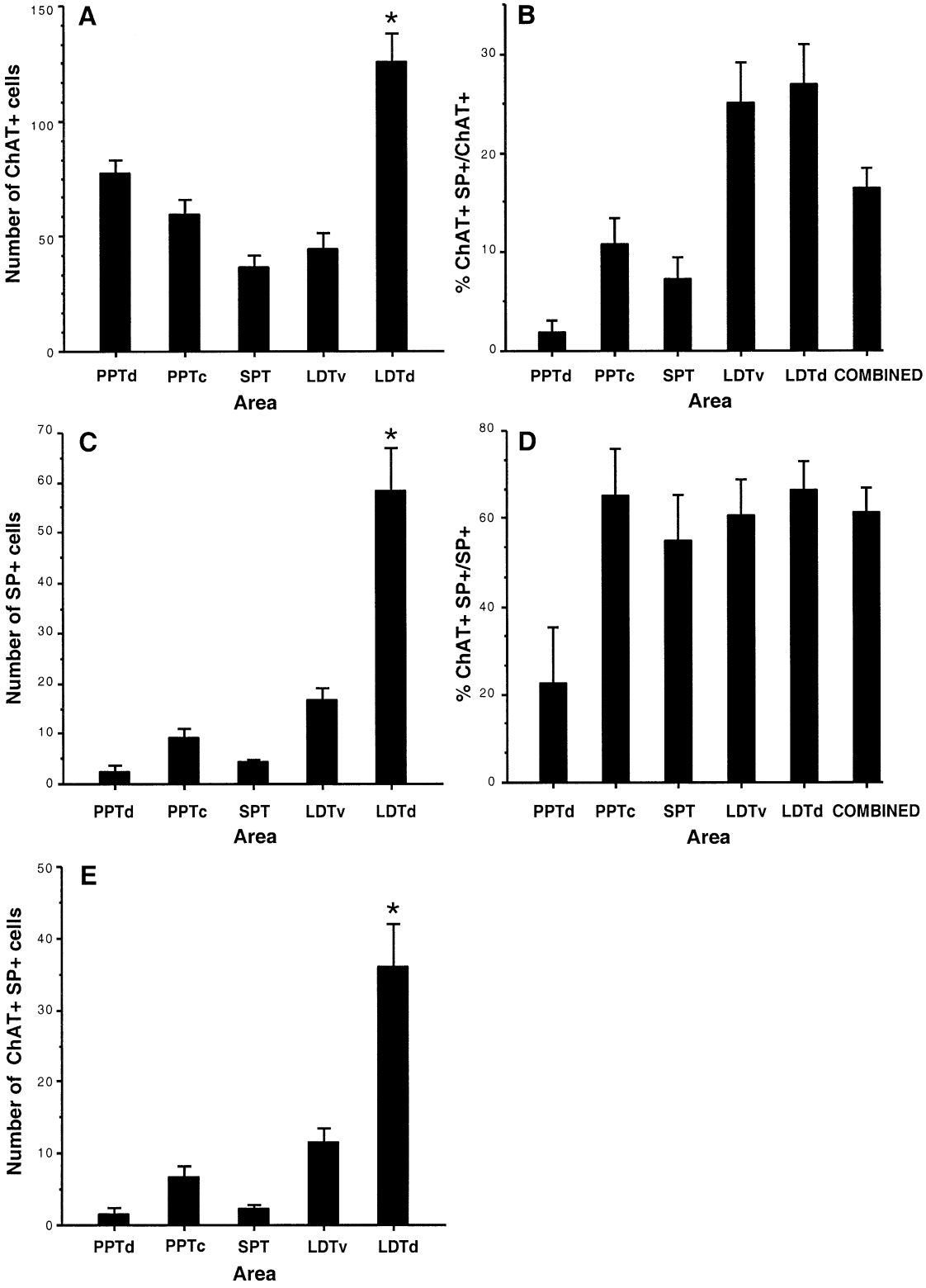

FIG. 5. The number of ChAT and/or SP-immunoreactive (+) neurons in the five subregions of the mesopontine tegmentum. See Methods for the methods of counting. (A and B) The number of ChAT+ neurons (A), and the percentage of ChAT+ neurons that are also SP+ (B). (C and D) The number of SP+ neurons (C), and the percentage of SP+ neurons that are also ChAT+ (D). (E) The number of ChAT+ and SP+ neurons. The data presented here are based on nine cases. $*P < 0.001$ between LDTd and each of the other regions.

subregions with ventral PRF injections, whereas, the number was similar across the subregions with dorsal PRF injections (Fig. 7E and F).

Electrophysiologlcal analysis

Effects of SP

The resting potential of PRF neurons was –63.9 ± 1.2 mV (n = 32). Application of 250 nM SP to cells while recording in current clamp mode depolarized all PRF cells examined (n = 23; Fig. 8A, 1). Substance P-induced inward current persisted in the presence of TTX (Fig. 8A, 1). As there were no detectable differences in responses of dorsal and ventral PRF neurons to SP nor were there differences attributable to age within the age range examined, data from these populations were pooled. The SP-induced depolarization was accompanied by a small but significant decrease in input resistance that is apparent in the high gain recording in Fig. 8B, 1: membrane potential and input resistance before and after SP administration were –64.3 ± 1.7 mV, 480.7 ± 39.4 MΩ, and –60.9 ± 1.8 mV, 451.7 ± 38.2 MΩ (n = 23), respectively, reflecting a 5.0 ± 1.0% change in the membrane potential and a 6.2 ± 1.5% change in input resistance. These changes were significant (P < 0.05). Consistent with these results, in voltage clamp mode, 250 nM SP induced an inward current of 100.7 ± 17.0 pA (n = 32) which was accompanied by an increase in whole cell conductance of 10.8 ± 1.3% (Fig. 9A); these changes were significant (P < 0.05). The change in conductance induced by SP is also evident in Fig. 11A (top), where the amounts of negative current necessary to step the cell to each of the stepped voltages in the presence of SP were greater than those necessary to step the cell to equivalent voltages in control conditions. The duration of these SP effects was 9.9 ± 1.4 min. Concentration–response curves revealed that electrophysiological effects of SP were concentration-dependent with EC_{50} of ≃ 250 nM (Fig. 10). Maximal inward current was induced by a concentration of 500 nM, and at higher concentrations the maximal inward current was reduced and was of a shorter duration (Fig. 10); the mechanisms underlying this attenuation were not explored in the present study.

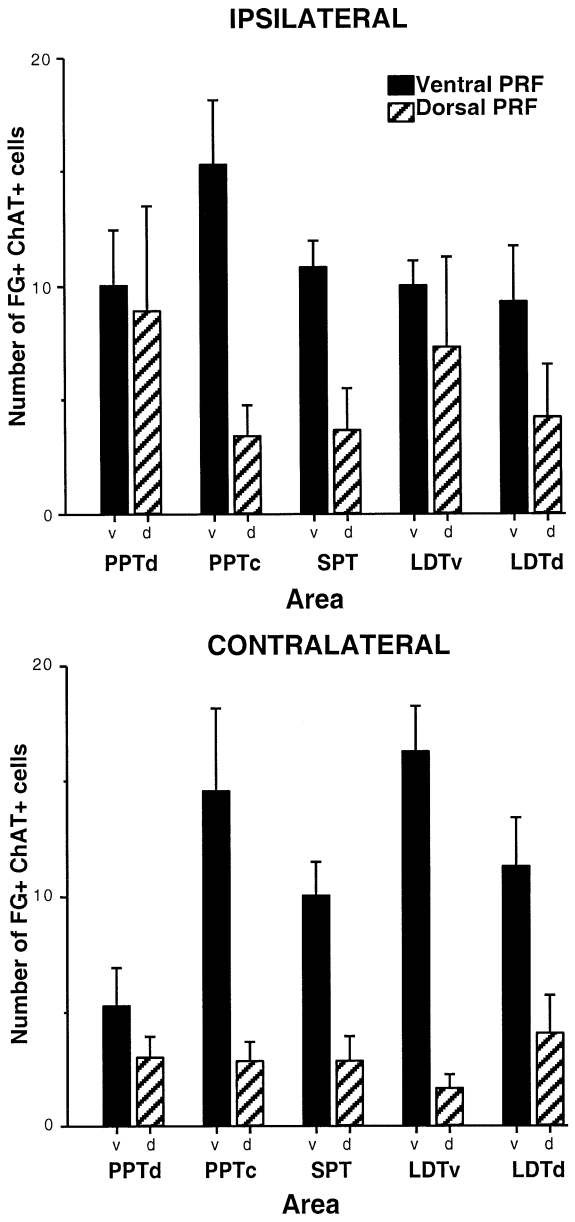

FIG. 6. The number of FG-labelled (+), ChAT-immunoreactive (+) neurons in five subregions of the mesopontine tegmentum ipsi- (A) and contralateral (B) to FG injections into the ventral (solid) and dorsal (hatched) PRF.

Measurement of the steady-state holding current in response to hyperpolarizing voltage steps from the holding potential of –60 mV to –130 mV, in 10 mV increments, revealed no reversal of SP-induced inward current at these potentials (n = 6; Fig. 9C). Substance P-induced inward current also did not reverse when the voltage was stepped from –60 mV to –30 mV (n = 4) (Fig. 9C). Although the control and SP curves appeared to approach convergence with progressively more positive voltages, the actual crossing did not occur within the analysed range (–130 mV to –30 mV; n = 10). Inadequate voltage clamp at potentials more positive than –30 mV precluded direct measurement of the reversal potential. In most cells (n = 16 out of 21), SP induced EPSP/EPSC activity with or without action potential generation (Fig. 9A and B, 2). The SP-induced inward currents were not significantly different in the presence of TTX. In 10 cells, SP was applied multiple times to determine the repeatability of these effects. Following 20 min of wash-out, the amplitude of the inward current evoked by SP was not significantly different than the previous application (P > 0.05) (Fig. 9B, 1–4).

In the presence of 1 μM of the SP antagonist (D-Arg^{1}, D-Pro^{2}, D-Trp^{7,9}, Leu^{11})-Substance P and TTX, the magnitude of the SP-induced inward current was reduced to 20.2 ± 5.5% of the control value (P < 0.05). Following washout of the antagonist, the response to SP recovered to 91.9 ± 1.5% of the control value (Fig. 10). These data combined with those showing that effects of SP persisted during blockade of muscarinic cholinergic receptors by atropine (see Results, Ionic species) suggest that SP was acting at a tachykinin/neurokinin receptor to mediate the aforementioned electrophysiological actions. No attempt was made to determine tachykinin/neurokinin receptor subtype(s) that mediated the effect.

Interactions between SP and cholinergic agonist effects

In a subset of PRF cells, the effects of sequential application of carbachol (1 μM) and SP (250 nM) were examined, with an appropriate washout period between treatments. It has been previously reported that carbachol depolarizes the majority of PRF neurons via closing of a K^+ channel (Greene *et al*., 1989). In agreement with these data, we found that carbachol induced either a depolarization (Fig. 8A, 2) or an inward current in 12 out of 16 PRF cells studied with an accompanying increase in resistance (Fig. 8B, 2). In 3 out of

3 cells studied in bridge mode, 1 μM carbachol elicited a depolarization of 3.4 ± 0.9 mV, and 250 nM SP depolarized these cells by 4.2 ± 0.7 mV. In 9 out of 13 cells studied in voltage clamp mode, carbachol elicited an inward current of 74.4 ± 25.0 pA and SP elicited an inward current of 89.7 ± 15.3 pA (Fig. 11A). In the minority of PRF neurons (4 out of 13) in which carbachol elicited an outward current of 250.3 ± 0.80 pA, SP induced an inward current of 120.3 ± 0.6 pA. Thus, SP elicited an inward current in PRF neurons irrespective of their response types to carbachol.

While persistence of SP effects in the presence of atropine and the SP antagonist is consistent with the interpretation that these two neuroactive substances act on different receptors, the depolarizing effects of activation of cholinergic and SP receptors upon PRF neurons could be mediated by a common set of ion channels or by distinct sets of channels. To examine this question, we studied the effects of concurrent application of SP and carbachol at the maximal effective concentration of 500 nM and 1 μM, respectively. The protocol involved administration of either SP or carbachol until maximal effects were observed, and then concurrent administration of the alternative agent such that their effects were superimposed, with the application order randomised. In those cells in which SP elicited depolarization, carbachol coapplication induced further inward current, and vice versa, indicating that effects were additive (SP alone, 54.0 ± 8.5 pA, carbachol alone, 82.0 ± 13.2 pA, SP and carbachol, 156.0 ± 21.4 pA, $P < 0.05$; $n = 4$; Fig. 11C, 1–3). In those cells in which carbachol elicited hyperpolarization, the effects of SP were attenuated in the presence of carbachol (SP alone, 68.8 ± 10.1 pA inward current; carbachol alone, 138.0 ± 34.6 pA

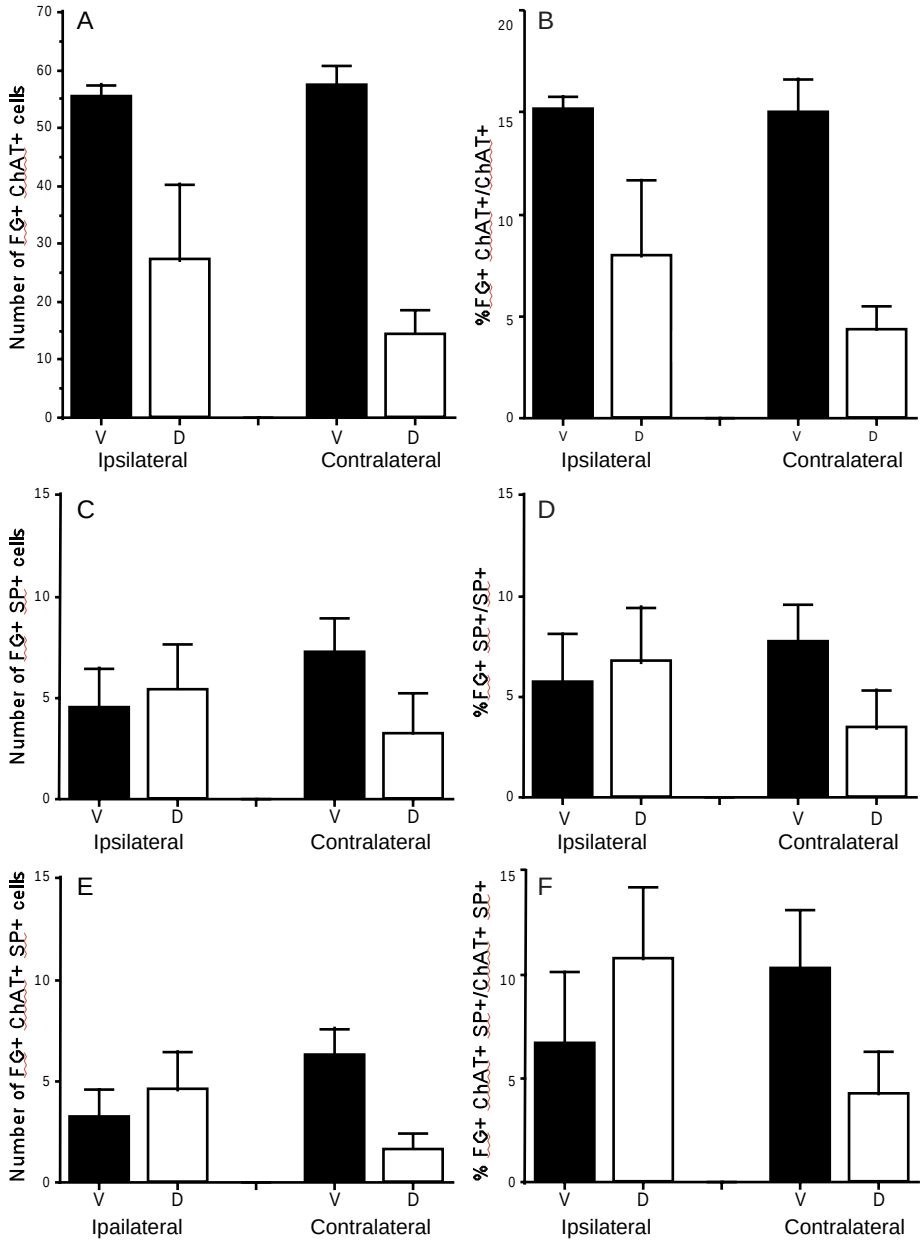

FIG. 7. The numbers and percentages of FG+ ChAT+ (A and B), FG+ SP+ (C and D), and FG+ ChAT+ SP+ (E and F) neurons after FG injections into the ventral (solid) and dorsal (open) regions of the PRF. *$P < 0.01$ between ventral and dorsal PRF for FG+ ChAT+ neurons (A and B).

outward current; SP and carbachol, 50.0 ± 49.2 pA outward current, $P < 0.05$; $n = 5$; Fig. 11C, 4 and 5). These data were consistent irrespective of the order of application. While not conclusive, these data suggest that carbachol and SP activate different channels and that their actions are additive.

Ion species mediating SP effects

Examination of the *I–V* curves revealed that the inward current induced by SP was due to an increase in conductance with a reversal potential more positive than –30 mV. A subset of PRF neurons exhibited prominent 'sag', attributed to activation of the hyperpolarization-activated inward conductance I_h as identified by the application of previously published protocols designed to elucidate the presence of this current (Kamondi *et al*., 1992). This I_h is mediated in part by K^+ ions. Substance P induced inward current in all PRF neurons tested regardless of the presence of I_h, indicating that I_h alone cannot explain the SP effect in all PRF neurons. However, to test the hypothesis that SP might depolarize a subset of PRF neurons by

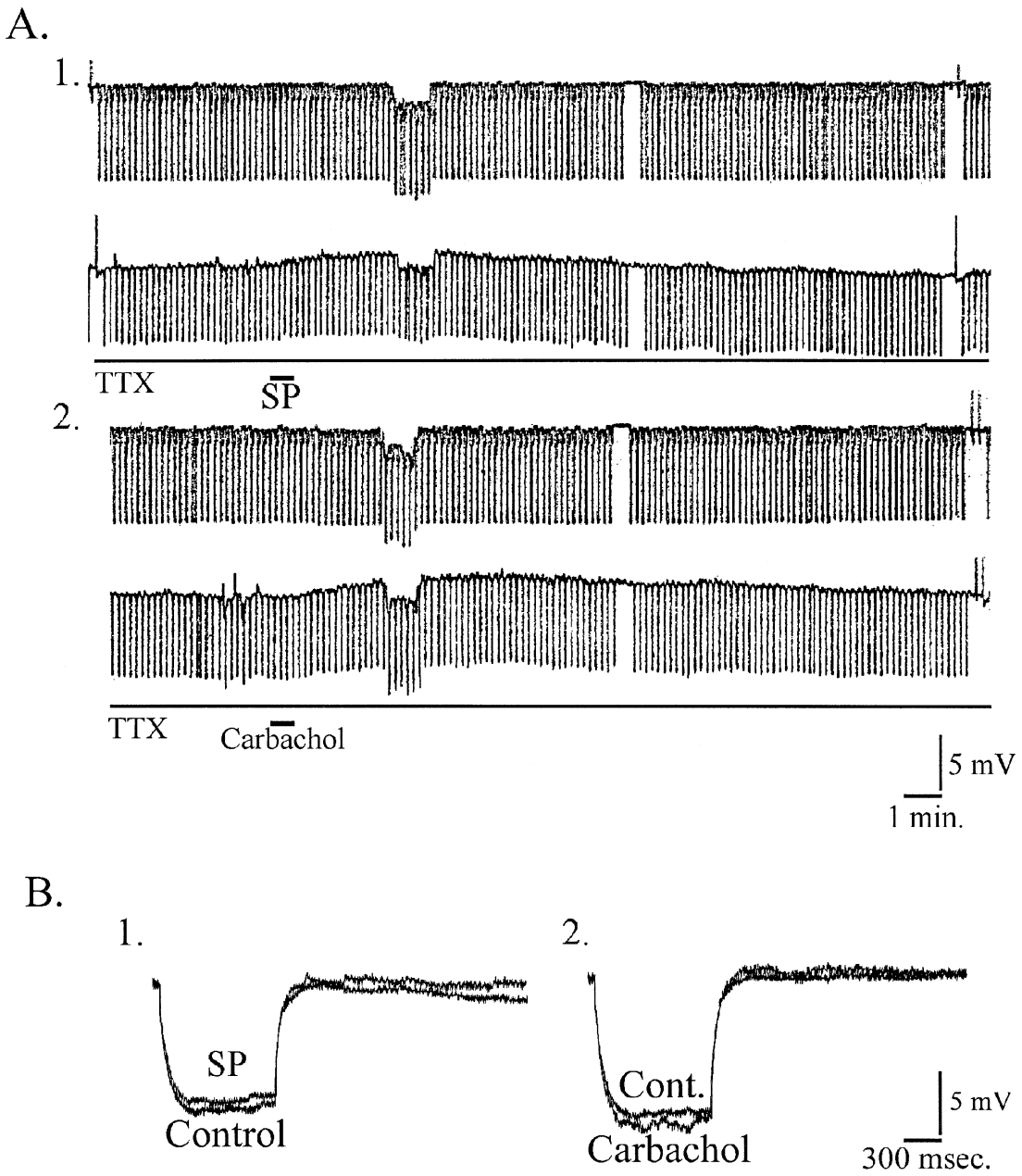

FIG. 8. Substance P (SP; 250 nM) depolarizes neurons in the REM sleep-induction zone of the PRF in the current clamp mode. (A) Top traces are current and bottom traces are voltage – downward going deflections result from the application of a brief 0.03 nA hyperpolarizing pulse in order to monitor input resistance. Recordings in A are from the same cell. Substance P evoked depolarization with a decrease in input resistance. (A_1) Depolarization persisted in the presence of 300 nM TTX indicating that effects of SP hinged upon action potential generation within the slice and that the current is being carried by TTX-insensitive postsynaptic conductances. (A_2) Carbachol 1 μM in the presence of TTX also depolarized this cell and reduced the conductance, as it did in the majority of cells in which SP induced depolarization and inward current. (B) Averaged responses (10 voltage responses) at high gain to hyperpolarizing current pulses (0.03 nA) in a cell at the same holding potential (–63.4 mV) showing a decrease in input resistance elicited by SP (B_1) and an increase in input resistance elicited by the cholinergic agonist carbachol (B_2).

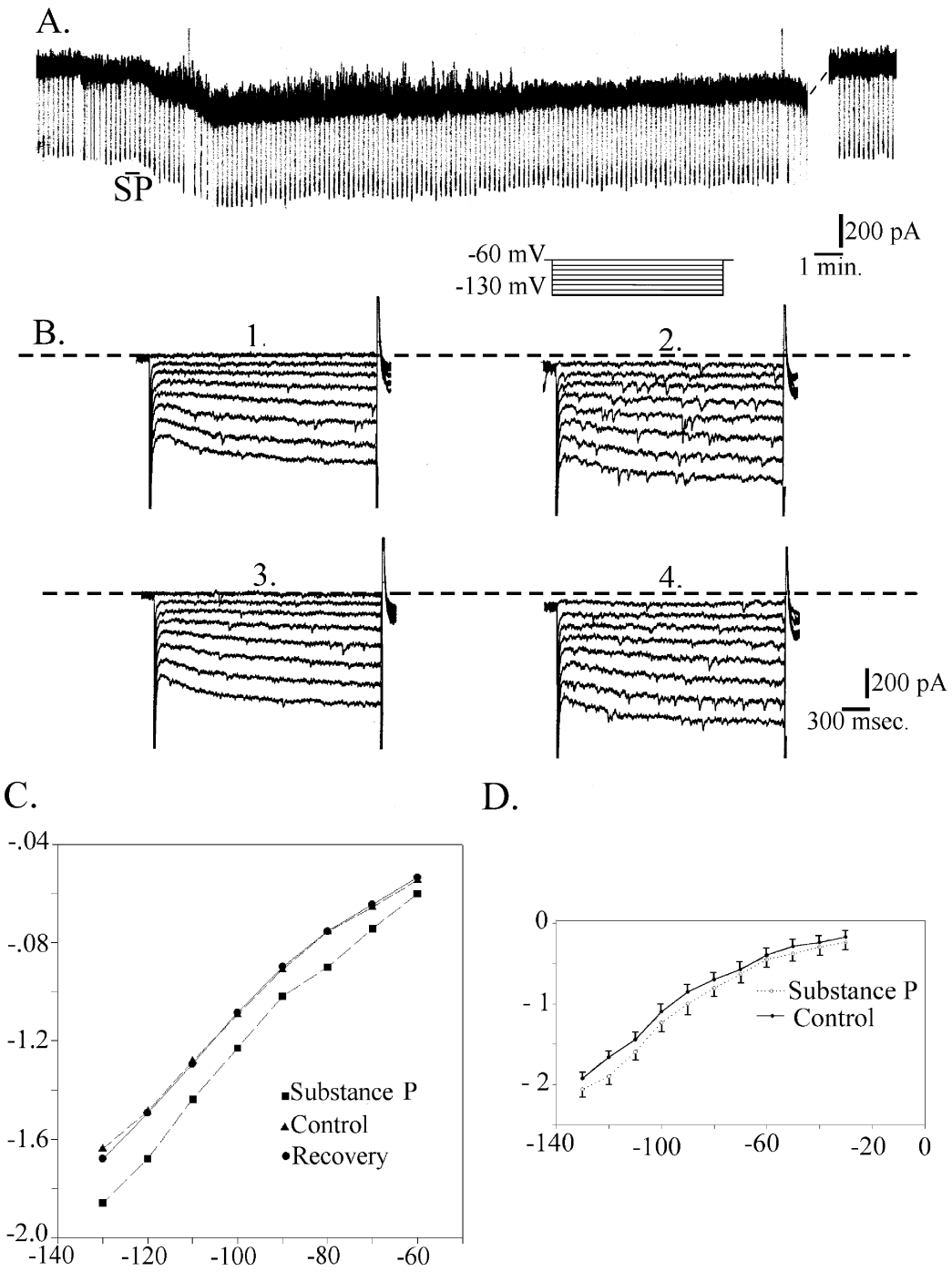

FIG. 9. Substance P evokes an inward current in voltage-clamp mode. (A) At the holding potential of –60 mV, SP elicited an inward current and an increase in conductance. An increase in EPSC activity is apparent in this trace and the traces of current steps in $B_{2,4}$. Downward deflections from the holding current in A reflect the stepping of the voltage from –60 mV to –90 mV in order to monitor conductance changes. B Current–voltage (*I–V*) relations measured by single electrode voltage clamp under control condition (B_1) and at the peak response to SP (B_2) in one cell. The cell was held at –60 mV and stepped from this potential to more negative voltages in –10 mV increments to a final voltage of –130 mV; increases in negative holding current necessary to hold the cell at –60 mV reflect the inward current induced by SP. The presence of an inwardly rectifying current in this cell is apparent in B.When previously published protocols (Kamondi *et al*., 1991) designed to reveal this current were applied (data not shown), this particular cell exhibited an I_h current which was not present in all PRF cells examined. The depolarizing effects of SP persisted in three cells in the presence of caesium in the bath, which blocks I_h (not shown), indicating that SP effects were not mediated by its effect on this conductance. Following wash-out from SP (B_3), reapplication of SP was as effective as the first application (B_4). (C) *I–V* curves are plotted from the steady-state values in one cell near the end of step protocols as in B. Substance P induced an inward current at all holding potentials tested (–60 to –130 mV) as indicated by the increase in negative holding current compared with control. (D) *I–V* curves generated from four cells in which the voltage was stepped from –130 to –30 mV. Substance P-induced inward current did not reverse in the voltage ranges tested. The slope conductance changed by 3.5% following SP application ($n = 4$) which corresponds well with the change in resistance measured utilizing the direct method (see Results). Horizontal axis in C and D is in mV and vertical axis is in nA.

acting upon I_h, we applied SP to three cells in the presence of 1 mM CsCl, which has been shown to block both I_h and an inwardly rectifying K^+ conductance in PRF neurons (Greene *et al*., 1989). The presence of I_h was examined and confirmed in one of these cells. CsCl did not significantly reduce the inward current induced by SP in either this or the other two cells ($P > 0.05$, data not shown).

The following observations suggest that an inward current induced solely by a decreased K^+ conductance is an unlikely explanation for the SP effect: (i) the inward current did not reverse around the calculated K^+ equilibrium potential of –103.6 mV; (ii) the inward current induced by SP was accompanied by an increase in conductance, rather than a decrease in conductance expected for a closing of K^+ channels; (iii) at the peak of the current induced by SP, the *I–V* relationship always displayed an inward shift compared to the control *I–V* at the voltage ranges tested indicating an associated conductance increase. This latter finding indicates that the inward current induced by SP cannot primarily be attributed to a decrease of a K^+ current normally maintained in these cells.

In order to test the hypothesis that SP depolarized cells by activation of a Ca^{2+} conductance, we examined the effects of SP upon PRF neurons in low Ca^{2+} ACSF. The amplitude of the SP-evoked inward current was not significantly changed in low Ca^{2+} ACSF (Fig. 12C); the average SP-induced depolarization and inward current in the presence of low Ca^{2+} solution were 8.3 ± 1.2 mV, and 76.6 ± 34.8 pA, compared with the control values in the same group of cells, 6.6 ± 1.1 mV, and 83.0 ± 39.6 pA (n = 4, 3). Low Ca^{2+} solution induced an inward current; therefore, effects of SP were examined in two cells following injection of negative current to bring the membrane potential to baseline and found to be not significantly different than in control conditions. These data not only indicate that the SP induced inward current is not substantially mediated by a Ca^{2+} conductance, but also demonstrate that the effect is not secondary to Ca^{2+}-dependent release of other transmitters.

We tested the hypothesis that a sodium current might be involved in mediation of the SP-induced current by choline substitution (n = 6). The depolarization and inward current evoked by SP in

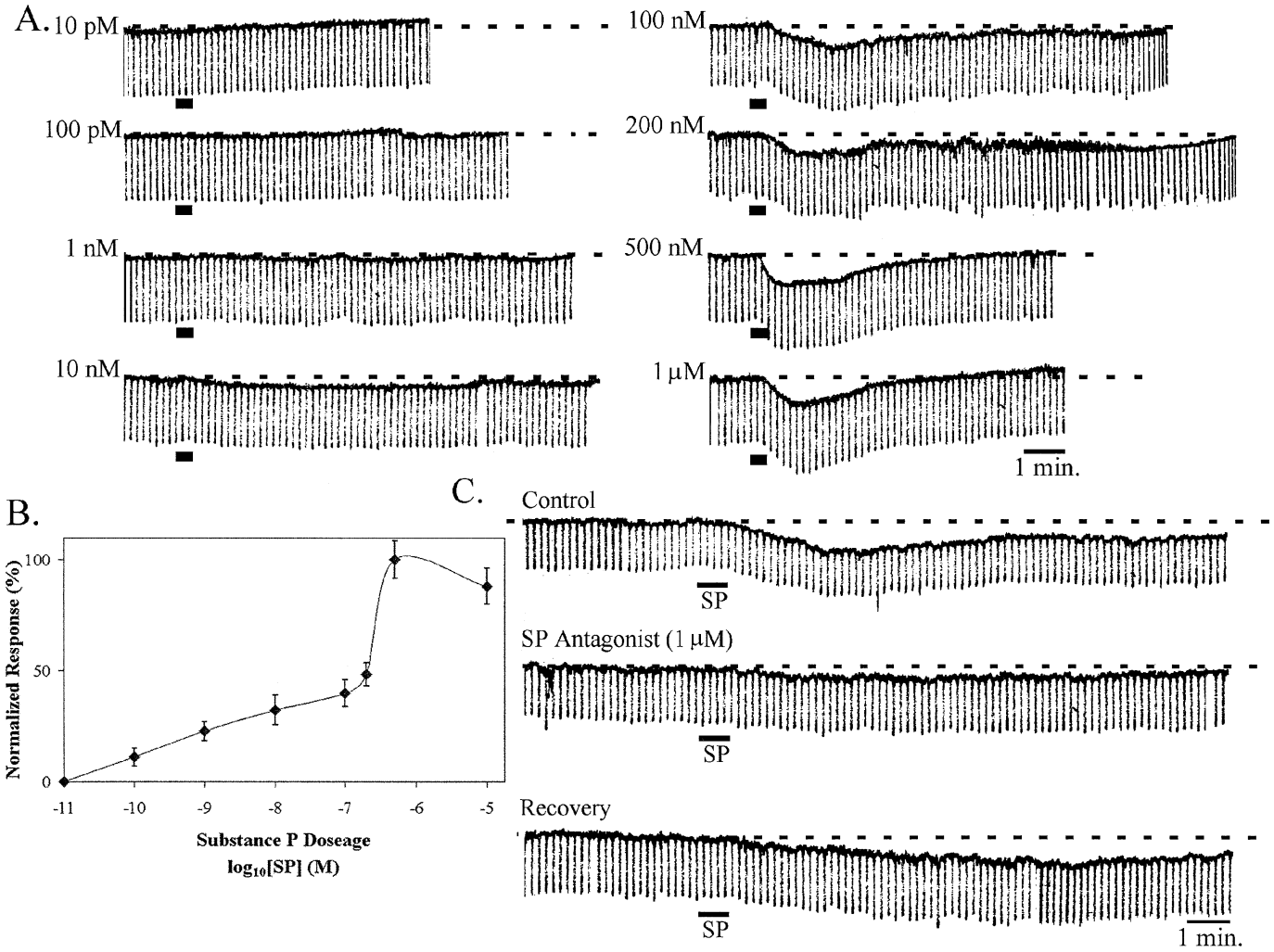

FIG. 10. Effects of SP are concentration-dependent. (A) The magnitude of inward current increases with increasing concentrations of SP from 10 pM to 500 nM. The highest concentration of SP tested (1 µM), however, tended to reduce the maximum current induced by this peptide and the duration of this effect. Bars indicate application of SP at the concentrations noted. (B) Dose response curve for SP-induced inward current evoked at a membrane potential of –60 mV (n = 4). Each point represents the mean normalized current induced by the peptide and error bars indicate the SEM. The EC_{50} was calculated at 250 nM and this was the concentration utilized in the majority of experiments, unless otherwise noted. The calculated concentration at which maximal effects on induction of inward current were achieved was 500 nM. (C) The effects of SP were antagonized by application of (D-Arg[1], D-Pro[2], D-Trp[7,9], Leu[11]) Substance P, an antagonist of SP at neurokinin receptors.

ACSF containing low Na^+ was significantly reduced in amplitude ($P < 0.05$) (Fig. 12A), from 6.8 ± 0.6 to 1.1 ± 0.1 mV ($n = 3$), and 114.0 ± 22.2 to 19.3 ± 11.9 pA ($n = 3$), respectively. Because choline substitution alone depolarized PRF neurons due to activation of muscarinic receptors, the experiments were repeated in the presence of 5 μM of atropine in three cells. Under these conditions, the SP-induced effects were not statistically different from those elicited in normal ACSF (Fig. 12B). It should be noted that the choline-mediated activation of muscarinic receptors (Wang & Aghajanian, 1987) on PRF cells in the presence of a low-Na^+ ACSF solution served as a control for nonspecific effects of Na^+ substitution and persistence of SP effects in atropine served as a control of effects of SP at muscarinic receptors.

Second messengers mediating SP effects

To test the hypothesis that production of cAMP may be involved in part in mediation of the response of PRF neurons to SP, the response to SP was evaluated in the presence of the membrane permeable cAMP-agonist, 8-bromo-cAMP. We reasoned that if the action of SP was mediated by an increase in intracellular levels of cAMP, the effects of SP should not be additive with those of 8-bromo-cAMP. In four cells, we first administered SP, which induced an inward current of 167.3 ± 112.9 pA. Following recovery from the initial SP application, 8-bromo-cAMP (1 mM) was administered for 15 min resulting in the production of an inward current of 55.6 ± 19.7 pA. Whilst the 8-bromo cAMP effect was maximal, SP was once again applied. In contrast to the effects seen with concomitant application

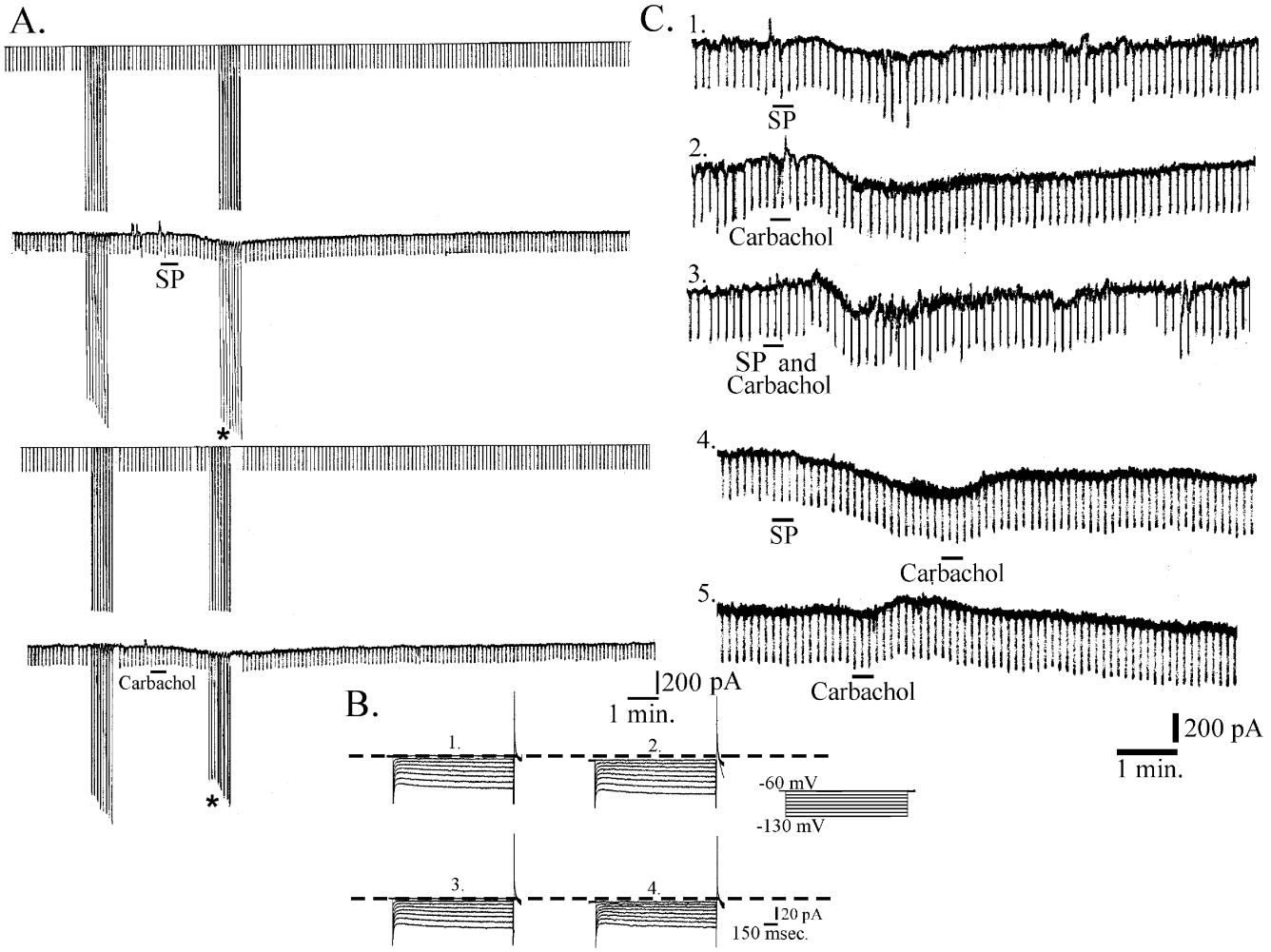

FIG. 11. Interactions of carbachol and SP on PRF cells. (A) In voltage clamp mode, SP was applied, and then following washout, carbachol. Downward deflections are in response to voltage steps from –60 to –130 mV in –10 mV increments from the holding potential of –60 mV. Top traces are voltage and bottom traces are current. Voltage was stepped from –60 mV to –130 mV; however, due to the high gain required to visualize the current, voltage deflections were clipped in the chart recording. As can be seen, the inward currents induced by these two agonists were similar in amplitude; however, as is apparent from the differing responses of this cell to negative voltage steps from the holding voltage of –60 mV in both conditions, the SP-induced inward current occurred with an increase in conductance (*), whereas, the carbachol induced current presented with a decrease in conductance (*). The latter is consistent with Greene *et al*. (1989) who demonstrated that carbachol depolarizes PRF cells by inhibition of a nonrectifying K^+ conductance. (B) High gain traces of the holding current for voltage steps of –10 mV from the holding potential of –60 mV taken from the cell in A before SP (B_1) and before carbachol (B_3), and after the administration. SP (B_2) and carbachol (B_4) induced a similar inward current as evident from the increase in negative holding current; however, the changes in conductance were opposite in direction. (C) Effects of carbachol and SP on induction of inward current were additive, in that the inward current induced by the combination of these agonists was greater than that seen by either one alone ($C_{1–3}$). These data support the conclusion that SP and carbachol are acting via different conductances to induce inward current in PRF cells. In those cells in which carbachol induced outward current, SP-induced inward current was superimposed on this effect (C_4 and C_5). In these studies, 500 nM of SP was utilized to achieve maximum effect of the peptide.

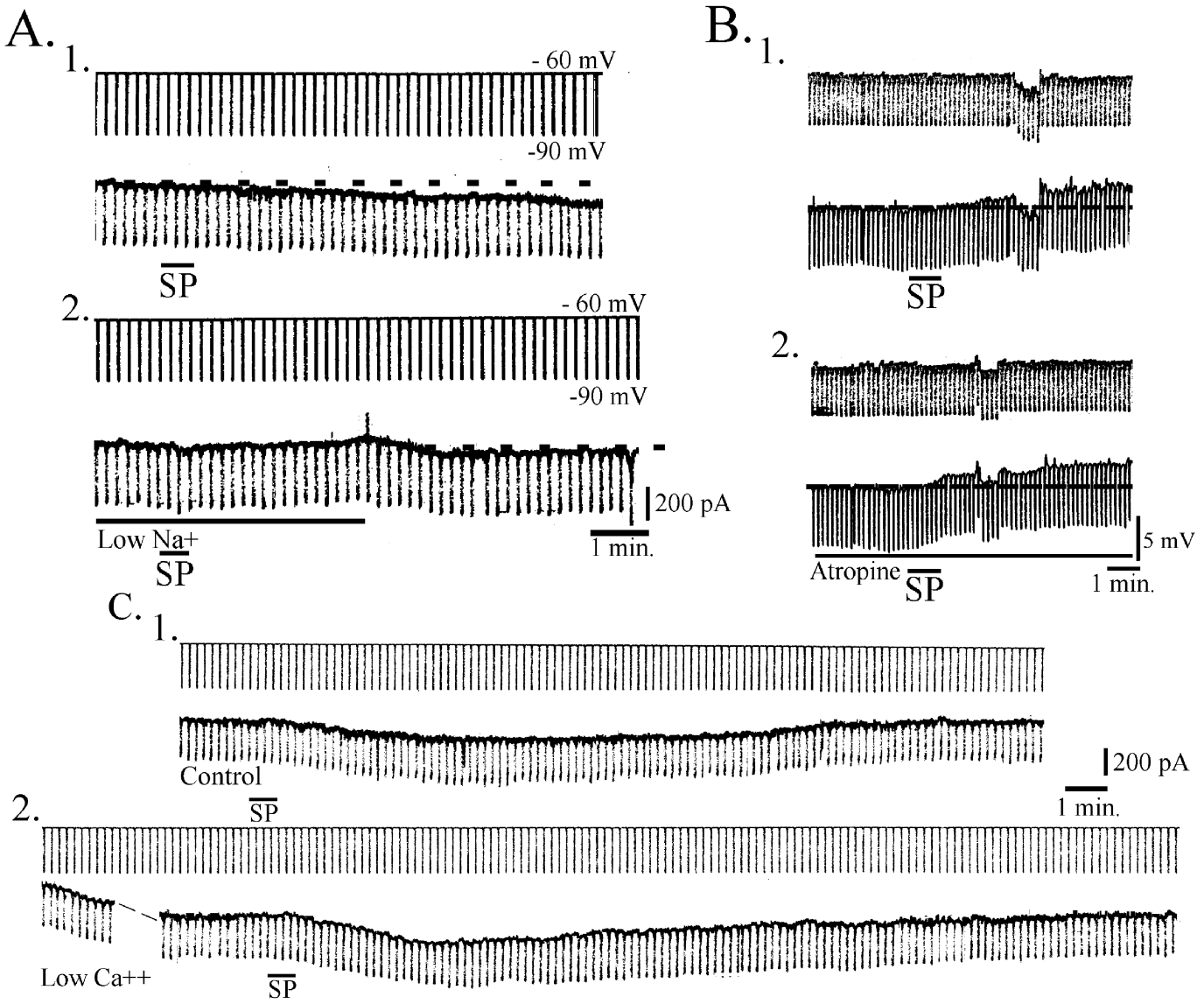

FIG. 12. The inward current activated by SP is carried at least in part by Na^+. (A) In voltage clamp, after obtaining the control response of a PRF cell to application of SP (A_1) and recovery, the ACSF was switched to that containing low Na^+ (A_2). The effect of SP was greatly attenuated. Top traces in A and C are voltage and bottom traces are current; downward deflections are the response to the stepping of the voltage from –60 mV to –90 mV in order to monitor conductance changes. (B) In the above experiment, atropine had been added to the low Na^+ ACSF to prevent depolarization of the membrane by choline ions. Therefore, effects of SP were examined in atropine-containing ACSF. Effects of SP examined in bridge mode in the presence of this muscarinic receptor antagonist (B_2) did not significantly differ from those in control ACSF (B_1). Top traces are current and bottom traces are voltage; downward deflections are the response to the application of 0.03 nA of hyperpolarizing current in order to monitor changes in input resistance. (C) In the presence of low Ca^{2+}, effects of SP (C_2) were not significantly different from those in normal ACSF (C_1). Low Ca^{2+} ACSF was applied throughout the duration of the recording shown in C_2. Low Ca^{2+} ACSF provides a synaptic blockade in the slice and, therefore, effectiveness of SP in inducing inward current in low Ca^{2+} ACSF also provides evidence that effects of SP are due to postsynaptic mechanisms. In the traces in A and (C) voltage steps from the holding potential of –60 mV to –90 mV are performed to monitor changes in conductance and in B the cell was injected with 0.03 nA of DC current during the depolarizing response to SP to return the cell to resting membrane potential so as to determine input resistance without contribution of voltage-sensitive conductances.

FIG. 13. Nonadditivity of the inward currents induced by 8-bromo-cAMP and SP. The inward current at –60 mV was measured in the voltage clamp mode. (A) Substance P was tested first, and after maximal induction of inward current and as the cell returned to the baseline potential, 8-bromo-cAMP was added to the perfusate. 8-bromo-cAMP induced an inward current which developed over 20 min; however, when SP was added again, the total inward current did not exceed that seen with SP alone. (B) In the presence of 2′5 dideoxyadenosine, an inhibitor of adenylate cyclase, SP induction of inward current was significantly attenuated. Following wash-out of the inhibitor, partial recovery (here 59%) of SP-induced current was obtained. (C) The cGMP agonist, 8-bromo-cGMP, attenuated the SP induced inward current. (D) The cGMP antagonist RP-8-pCPT-cGMPs did not diminish the response to SP. These data indicate that the cGMP second messenger system is not implicated in the induction of inward current by SP and are consistent with the interpretation that concurrent activation of the cGMP second messenger pathway with those activated by SP, diminishes the SP responses. Application of SP is indicated by bars underneath traces. Widely spaced dotted lines represent baseline holding current; more narrowly spaced dotted lines represent the shift in baseline with 8-bromo-cAMP, 8-bromo-cGMP and RP-8-pCPT-cGMPs in A, C and D, respectively. Horizontal bar represents 1 min and vertical bar represents 150 pA of current.

of carbachol and SP (above), coapplication of 8-bromo-cAMP and SP produced an inward current of 71.4 ± 75.2 pA, which was not significantly different from that seen with SP alone (Fig. 13). These data support that cAMP is involved in the SP-induced current.

To further test the hypothesis that adenylate cyclase (AC) is involved in generation of the SP-induced inward current, following wash-out of the first application of SP, to establish baseline effects, SP was applied in the presence of the AC inhibitor, 2,5 dideoxyadenosine.

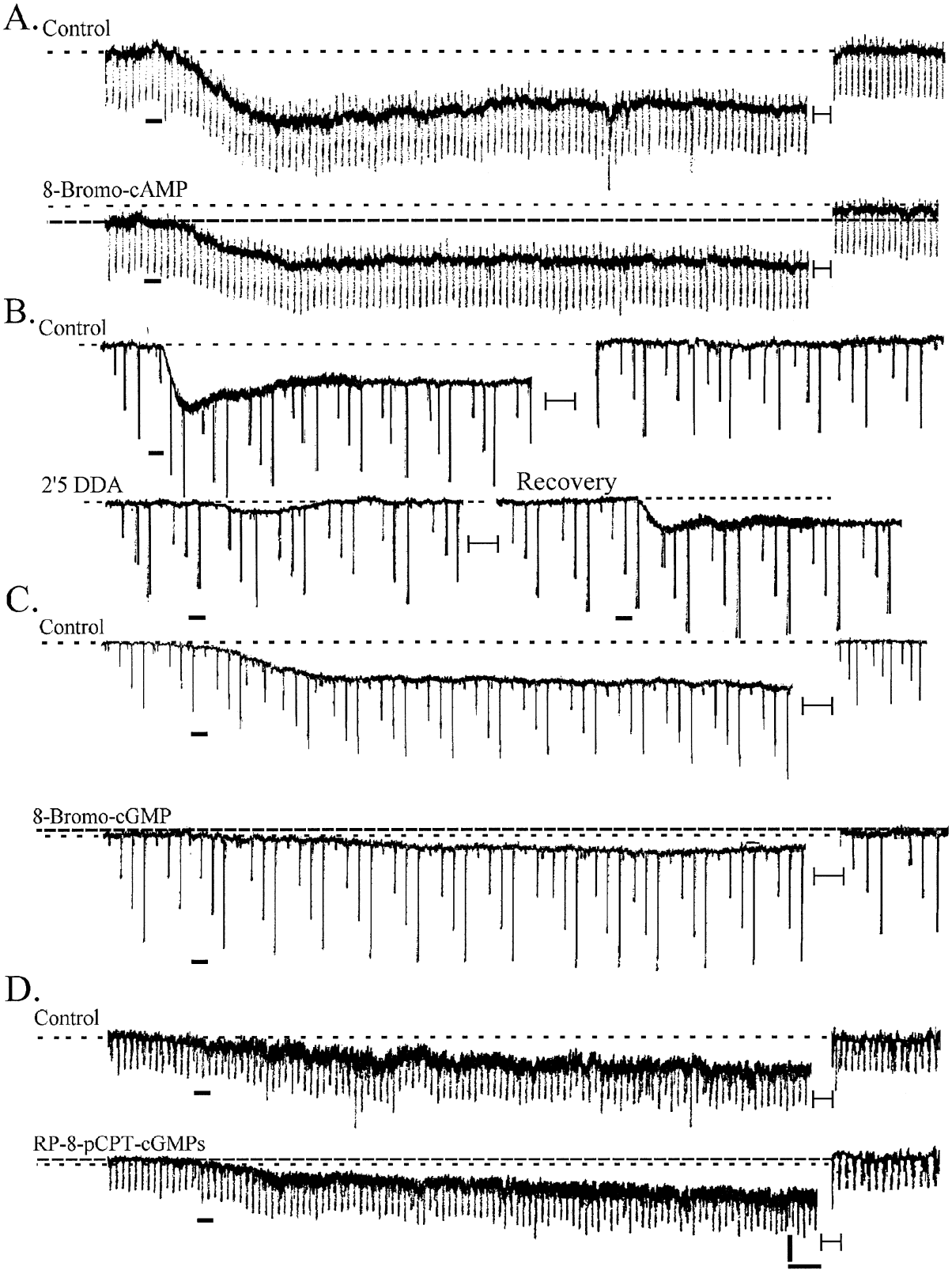

In the presence of 2,5 dideoxyadenosine (10 μM), SP-induced inward current was either abolished ($n = 3$ out of 5) or greatly attenuated to 19.8 ± 0.6% of the maximal current ($n = 2$ out of 5) (Fig. 13B). In two cells in which recordings were maintained following several minutes of wash-out of 2,5 dideoxyadenosine, the SP effect recovered to a mean of 79% of its initial level. These findings support the hypothesis that intracellular accumulation of cAMP is involved in the electrophysiological actions of SP on PRF neurons.

It has been previously suggested that increases in cGMP may be involved in SP-mediated effects in some neuronal types (Mistry & Vijayan, 1987). To test the hypothesis that increased cGMP levels might be involved in the SP-mediated inward current in PRF cells, we examined the effects of SP either in the presence of the cGMP agonist, 8-bromo-cGMP or RP-8-pCPT-cGMPs, an inhibitor of cGMP-dependent kinases. We found that 8-bromo-cGMP induced an outward current in all cells examined and the SP induced inward current was attenuated in the presence of this outward current ($n = 4$ out of 4; Fig. 13). Moreover, in the presence of 10 μM RP-8-pCPT-cGMPs, the amplitude of the SP induced inward current was not significantly different than under control conditions in the same cells ($n = 3$, $P > 0.05$; Fig. 13). These data suggest that cGMP does not mediate the effects of SP upon PRF cells.

Discussion

The main findings of the present study are that SP is present in a subpopulation of mesopontine cholinergic neurons that send descending projections to REM sleep-induction regions of the PRF, and that SP consistently depolarizes PRF neurons through a mechanism which is distinct from those that mediate effects of cholinergic receptor agonists. The SP-induced depolarization involves activation of a non-TTX-sensitive cation current(s) secondary to an increase in intracellular cAMP. The anatomical and physiological studies were conducted using animals of different ages for technical reasons and age-related differences were not determined. In light of the implication of the cholinergic projections from the mesopontine tegmentum–PRF in the generation of REM sleep (for reviews, see Steriade & McCarley, 1990; Semba, 1999), and state-dependent release of acetylcholine in the REM sleep-induction regions of the PRF (Kodama *et al*., 1990; Leonard & Lydic, 1997), the present findings are consistent with the possibility that natural release of SP, along with acetylcholine, in the PRF may play a role in both triggering the onset of REM sleep and maintaining the state during the bout of REM sleep.

Cholinergic projections to the PRF

The anatomical results presented here extend previous findings (Vincent *et al*., 1983; Sutin & Jacobowitz, 1990) by providing quantitative analysis showing that 16% of all cholinergic neurons in the mesopontine tegmentum contain SP, and that the majority (64%) of these neurons are located caudally within the mesopontine tegmentum, i.e. in the LDTd. Furthermore, up to 11% of SP-containing cholinergic neurons in the mesopontine tegmentum are found to project to REM sleep-induction regions of the PRF. Although the quantitative analysis indicates that these neurons represent a relatively small proportion (less than 5%) of the entire cholinergic cell population in the mesopontine tegmentum, these percentages are likely to be underestimated for technical reasons, including the use of rigorous criteria to exclude false positives as well as limited antibody penetration, and the actual percentages are probably higher. In addition, neuropeptides tend to act at lower concentrations than do classical neurotransmitters (e.g. Kohlmeier & Reiner, 1999; Agnati *et al*. 2000), and it is possible that relatively small amounts of SP released by a subset of cholinergic neurons might still have significant effects through direct synaptic mechanisms, and/or via volume transmission (Agnati *et al*. 2000) by diffusing from the original site of release to activate specific receptors present on adjacent PRF neurons. The significance of a high percentage of SP-containing cholinergic neurons specifically in the LDTd is not clear. However, this would imply that structures innervated by LDT cholinergic neurons would have higher probability of SP corelease than those innervated by PPT cholinergic neurons. The fact that a subpopulation of SP-containing cholinergic neurons appear to project to the PRF suggests that many SP-containing cholinergic neurons might project elsewhere in the brain. Whether some of these remaining, or the PRF-projecting, SP-containing cholinergic neurons project to the thalamus (Oakman *et al*., 1999) was not determined in the present study.

Our data demonstrate for the first time that the ventral region of the PRF is innervated by a greater number of mesopontine cholinergic neurons than the dorsal PRF region. The ventral PRF tracer injection sites roughly corresponded to the sites of carbachol injections that have been reported to be most effective in inducing REM sleep in rats (Gnadt & Pegram, 1986; Bourgin *et al*., 1995; Deurveilher *et al*., 1997), although some of the effective sites in these studies were located more dorsally and rostrally as well. The dorsal PRF injection sites, on the other hand, corresponded more closely to the effective sites reported in a number of studies using cats (Baghdoyan *et al*., 1984; Vanni-Mercier *et al*., 1989; Yamamoto *et al*., 1990), and were also similar to the tracer injection sites in our previous anatomical studies in rat (Semba *et al*., 1990; Semba, 1993). More recent studies using cats, however, have reported that the most effective sites were located more ventrally in the rostral PRF (Reinoso-Suárez *et al*., 1994; Garzon *et al*., 1998), and these sites correspond roughly to the ventral PRF sites in the present study. Whether the dorsal and the ventral PRF regions in cat also show differences in the density of cholinergic projections remains to be investigated. However, it appears that in both rat and cat, the most effective sites include the regions medial and ventromedial to the motor trigeminal nucleus approximately at the junction of the rostral and caudal pontine reticular nuclei, and the present study showed that in the rat, this area receives heavier cholinergic projections than do more dorsolateral and rostral PRF regions.

In addition to the heavier cholinergic innervation of the ventral than the dorsal PRF, we have found that the projections to the dorsal PRF show ipsilateral dominance whereas those to the ventral PRF were bilateral. The SP-containing projections also showed organizational differences; SP-containing cholinergic neurons projecting to the ventral PRF were located most numerously in the LDTv, whereas, those innervating the dorsal PRF tended to be more evenly distributed across the mesopontine tegmentum. The ventral and dorsal injection sites were located within a region from the caudal part of the oral pontine reticular nucleus to the rostral part of the caudal pontine reticular nucleus; however, within this region the ventral injection sites as a group tended to be slightly more caudal than the dorsal injection sites. The oral and caudal pontine reticular nuclei are known to have generally similar, but some differential, efferent (Jones & Yang, 1985; Vertes & Martin, 1988; Reinoso-Suárez *et al*., 1994) and afferent connections (Shammah-Lagnado *et al*., 1987). The present findings of differential cholinergic innervation of the ventral and dorsal PRF add to the list of various organizations of ipsilateral and contralateral descending projections from PPT and LDT cholinergic neurons to pontine and medullary structures (Shammah-Lagnado

et al., 1987; Rye *et al*., 1988; Woolf & Butcher, 1989). Taken together, these anatomical differences further suggest distinct anatomical organization of the ventral and dorsal PRF in the rat and their functional implications for REM sleep control remain to be investigated.

Substance P-induced depolarization and its mechanisms

In the present study we demonstrate that SP has a dramatic, direct, depolarizing effect on all dorsal and ventral PRF neurons studied. These effects were dose-dependent, antagonized by a SP antagonist, and mediated by an increase in intracellular cAMP. SP has been shown to activate voltage-dependent Ca^{2+} channels, voltage-dependent K^+ currents, Cl^- conductances, hyperpolarization-activated cation conductances, voltage-dependent Na^+ channels and nonselective cation channels (Adams *et al*., 1983; Stanfield *et al*., 1985; Bley & Tsien, 1990; Shen & North, 1992; Bertrand & Galligan, 1994). We have examined these and other possibilities in order to explain the ionic mechanisms of the SP-induced depolarisaton in the present study.

The *I–V* relationship obtained with SP did not intersect with that obtained under control conditions over the range of membrane potentials of –130 mV to –30 mV suggesting that the inward current is due to an increase in conductance(s) whose reversal potential is positive to –30 mV. A role for TTX-sensitive voltage-dependent sodium channels can be ruled out in the present study because the SP-induced inward current persisted in the presence of TTX. The significant involvement of a K^+ conductance was ruled out because the reversal potential for K^+ is much more negative than the projected reversal potential (> –30 mV) of the SP-induced current. In addition, carbachol has been shown to induce depolarization or hyperpolarization of PRF neurons via closing or opening of a K^+ channel, respectively (Greene *et al*., 1989), and the additive effects of carbachol and SP are also consistent with the interpretation that depolarization induced by SP is not primarily due to its effects on K^+ channels. Substance P had no effect on I_h, a K^+/Na^+ conductance present in a subset of PRF neurons. This current was not mediated by an increase in a Cl^- conductance because while the calculated reversal potential of Cl^- (–32 mV) is more positive than the resting potential of PRF neurons (–63.9 mV), the SP-induced current did not reverse around – 30 mV.

Ion substitution studies taken together with the lack of crossing of control and SP-induced current *I–V* curves at the potentials tested led us to conclude that under physiological conditions, while it may not be the only current involved, a conductance carried by Na^+ and attributable to opening of TTX-insensitive cation channels which may be nonspecific accounts for at least a part of the inward current observed during SP application in the case of PRF neurons at resting membrane potentials. However, because low Na^+ solutions did not entirely abolish SP-induced currents, it is likely that Na^+ are not the only ion species mediating SP effects. This conclusion is consistent with the findings that SP activates nonselective cation channels on rat locus coeruleus and sensory neurons (Shen & North, 1992; Koyano *et al*., 1993; Inoue *et al*., 1995). Detailed elucidation of other ionic species or channels that may contribute to SP-induced current was beyond the scope of the present report.

We found that an antagonist of SP reduced the response to SP by 80%, suggesting that tachykinin/neurokinin receptor predominantly mediated the response, and this study began to explore the second messenger system(s) involved in mediating effects of SP. The mammalian tachykinin system consists of three distinct peptides, SP, substance K and neurokinin and possesses three corresponding types of receptors; each peptide is able to bind to all the three receptors albeit with differing affinities. Each receptor subtype has been shown to activate a variety of signal transduction mechanisms in neurons, including the AC/cAMP and phospholipase C (PLC)–inositol phosphate pathways (Womack *et al*., 1985; Merritt & Rink, 1987; Yoshimasa *et al*., 1987; Horstman *et al*., 1988; Peralta *et al*., 1988; Nakajima *et al*., 1992; Catalan *et al*., 1995). Substance P has been shown to bind to a tachykinin receptor coupled directly to both AC and phospholipase C resulting in cAMP formation and stimulation of phosphatidyl inositol hydrolysis, respectively (Nakajima *et al*., 1992). The ability of SP to stimulate increases in the intracellular concentrations of cAMP has been well-documented in neurons of rat brain (Duffy & Powell, 1975; Mistry & Vijayan, 1987; Moser, 1990; Palkovits *et al*., 1990; Mitsuhashi *et al*., 1992). These data coupled with the finding of a cAMP-induced inward current in PRF neurons in the REM-induction zone (Kohlmeier & Reiner, 1999) suggested that the SP-induced inward current may be at least in part dependent on production of cAMP.

In support of the hypothesis that cAMP is involved in SP effects, we found that effects of SP and 8-bromo-cAMP were not additive. However, interestingly, the total current induced was of a lower magnitude than that induced on average by SP alone. When applied to a slice, 8-bromo-cAMP at the concentrations utilized probably has a multiplicity of effects unrelated to mechanisms activated by SP, which might result in a countering of SP effects. This might explain the reduction of the amplitude of the SP-induced current in the presence of 8-bromo-cAMP. The main conclusion that can be drawn from the present data is that the cumulative effects of 8-bromo-cAMP and SP were not greater than effects of SP alone. Had cumulative effects been found to be greater than summation of individual effects, it would have indicated that SP effects are not mediated by cAMP. Further supporting a role of cAMP in SP-induced effects, we found that an AC inhibitor either abolished the inward current induced by SP or attenuated it to 20% of the control level. Taken together, our data suggest that activation of the AC/cAMP pathway via stimulation of a tachykinin receptor is principally involved in mediation of SP-induced inward current. Our preliminary results indicate that the PKC agonist, phorbol 12-myristate 13-acetate (PMA), induced an inward current in PRF cells with an increase in conductance, and that in the presence of this PKC agonist, the SP-induced inward current was potentiated (K. A. Kohlmeier & P. B. Reiner, unpublished observations). From the present data, it is clear that AC dependent mechanisms are primarily responsible for the SP-induced inward current in PRF cells, with the role of the PLC second messenger system requiring further investigation.

Although it has been reported previously that SP has activity at acetylcholine receptors (Anderson *et al*., 1993; Guevara Guzman *et al*., 1993; Valenta *et al*., 1993; Holzer & Maggi, 1994; Sastry, 1995; Costello *et al*., 1998) and that other peptides that enhance REM sleep following injection into the mPRF, such as vasoactive intestinal polypeptide (VIP; Bourgin *et al*., 1999) and pituitary adenylate cyclase activating polypeptide (PACAP; Ahnaou *et al*., 1999, 2000), were found to mediate their effects via interactions with muscarinic receptors, it is unlikely that the effects of SP are mediated by such receptors for the following reasons. The SP-induced effects persisted in the presence of the muscarinic receptor antagonist atropine, were attenuated in the presence of a SP antagonist, and were additive to effects seen with stimulation of cholinergic receptors by carbachol. Greene *et al*. (1989) demonstrated that carbachol induces inward current in PRF cells via non-M_1 muscarinic receptor inhibition of a K^+ conductance, whereas carbachol-activated outward current has been reported to be mediated via activation of an inwardly rectifying K^+ conductance via activation of a non-M_1 conductance (Gerber *et al*.,

1991). The additivity of SP and carbachol effects suggests that carbachol and SP act via different channels to elicit their effects on membrane potential, and that SP does not affect the nonrectifying K^+ or inwardly rectifying K^+ conductance activated by carbachol in PRF cells. Rather different results were obtained in the rat locus coeruleus where Shen & North (1992) reported that occlusion of inward current occurred with concurrent application of SP and muscarine. Both SP binding sites (Buck *et al*., 1984) and SP receptor immunoreactivity have been observed in the PRF (Nakaya *et al*., 1994). Our electrophysiological findings suggest for the first time that the SP receptors demonstrated by these latter studies to be present in the PRF are functionally capable of inducing electrophysiological effect upon release of SP.

Functional significance

Substance P was found to be present in cholinergic mesopontine neurons that project to the REM-induction zone in the PRF. Several lines of evidence suggest that SP and acetylcholine could be concurrently released by axon terminals of these mesopontine neurons, especially just preceding, and during the period of REM sleep to initiate and maintain REM sleep. First, just prior to REM sleep onset and continuing during the state, most neurons in the LDT and PPT increase firing rate, and an unidentified population of LDT neurons switch from a tonic firing to a burst firing pattern (Nelson *et al*., 1983; El Mansari *et al*., 1989; Steriade *et al*., 1990a,b; Kayama *et al*., 1992). Peptide release from neurons has been shown to be facilitated particularly by a high frequency firing profile (Lundberg & Hökfeldt, 1983). Therefore, while neither the transmitter phenotype nor projections of these neurons are known, the change in activity of LDT and PPT neurons at the onset of REM sleep is certainly consistent with the possibility that SP is coreleased in the PRF prior to and during REM sleep. Furthermore, we found that the effects of carbachol and SP on PRF neurons were additive. During naturally occurring REM sleep, the majority of PRF neurons within the REM-induction zone depolarize by 7–10 mV (Ito & McCarley, 1984) and cholinergic agonists depolarize the majority of PRF cells within this region (Greene *et al*., 1989). These and the current findings suggest that the concurrent release of SP and acetylcholine during REM sleep would lead to greater excitation of PRF neurons than can be achieved by acetylcholine alone. Taken together, the data in the present report provide strong experimental and mechanistic support for the hypothesis that SP release in the PRF plays a role in regulation of REM sleep. This hypothesis would be strengthened further by demonstration of release of SP (and acetylcholine) during REM sleep as well as behavioural effects of SP microinjections into the PRF.

Acknowledgements

Research was supported by grants from the Canadian Institutes of Health Research (MT-14451) and NSERC 217301–99. K. A. K was supported by a postdoctoral fellowship from the National Sleep Foundation (USA).

Abbreviations

AC, adenylate cyclase; aCSF, artificial cerebrospinal fluid; AHP, after-hyperpolarization; ANOVA, analysis of variance; ChAT, choline acetyltransferase; FG, fluorogold; FITC, fluorescein isothiocyanate; LDTd, laterodorsal tegmental nucleus, dorsal part; LDTv, laterodorsal tegmental nucleus, ventral part; PPTc, pedunculopontine tegmental nucleus pars compacta; PPTd, pedunculopontine tegmental nucleus pars dissipata; PRF, pontine reticular formation; REM, rapid eye movement; SP: substance P; SPT, subpeduncular tegmental nucleus; VIP, vasoactive intestinal polypeptide.

References

Adams, P.R., Brown, D.A. & Jones, S.W. (1983) Substance P inhibits the M-current in bullfrog sympathetic neurones. *Eur. J. Pharmacol.*, **79**, 330–333.

Agnati, L.F., Fuxe, K., Nicholson, C. & Syková, E. (2000) Volume transmission revisited. *Prog. Brain Res*., **125**, Elsevier, Amsterdam, pp. 470.

Ahnaou, A., Basille, M., Gonzalez, B., Vaudry, H., Hamon, M., Adrien, J. & Bourgin, P. (1999) Long-term enhancement of REM sleep by the pituitary adenylyl cyclase-activating polypeptide (PACAP) in the pontine reticular formation of the rat. *Eur. J. Neurosci.*, **11**, 4051–4058.

Ahnaou, A., Laporte, A.M., Ballet, S., Escourrou, P., Hamon, M., Adrien, J. & Bourgin, P. (2000) Muscarinic and PACAP receptor interactions at pontine level in the rat: significance for REM sleep regulation. *Eur. J. Neurosci.*, **12**, 4496–4504.

Anderson, J.J., Chase, T.N. & Engber, T.M. (1993) Substance P increases release of acetylcholine in the dorsal striatum of freely moving rats. *Brain Res.*, **623**, 189–194.

Baghdoyan, H.A., Rodrigo-Angulo, M.L., McCarley, R.W. & Hobson, J.A. (1984) Site-specific enhancement and suppression of desynchronized sleep signs following cholinergic stimulation of three brainstem regions. *Brain Res.*, **306**, 39–51.

Bertrand, P.P. & Galligan, J.J. (1994) Contribution of chloride conductance increase of slow EPSC and tachykinin current in guinea-pig myenteric neurones. *J. Physiol. (Lond.)*, **481**, 47–60.

Bley, K.R. & Tsien, R.W. (1990) Inhibition of Ca^{2+} and K^+ channels in sympathetic neurons by neuropeptides and other ganglionic transmitters. *Neuron*, **2**, 379–391.

Bourgin, P., Ahnaou, A., Laporte, A.M., Hamon, M. & Adrien, J. (1999) Rapid eye movement sleep induction by vasoactive intestinal peptide infused into the oral pontine tegmentum of the rat may involve muscarinic receptors. *Neuroscience*, **89**, 291–302.

Bourgin, P., Escourrou, P., Gaultier, C. & Adrien, J. (1995) Induction of rapid eye movement sleep by carbachol infusion into the pontine reticular formation in the rat. *Neuroreport*, **6**, 532–536.

Bourgin, P., Lebrand, C., Escourrou, P., Gaultier, C., Franc, B., Hamon, M. & Adrien, J. (1997) Vasoactive intestinal polypeptide microinjections into the oral pontine tegmentum enhance rapid eye movement sleep in the rat. *Neuroscience*, **77**, 351–360.

Buck, S.H., Helke, C.J., Burcher, E., Shults, C.W. & O'Donohue, T.L. (1984) Pharmacologic characterization and autoradiographic distribution of binding sites for iodinated tachykinins in the rat central nervous system. *Peptides*, **7**, 1109–1120.

Catalan, R.E., Martinez, A.M., Aragones, M.D., Hernandez, E., Liras, A. & Miguel, B.G. (1995) Further studies on the mechanism of action of substance P in rat brain, involving selective phosphatidylinositol hydrolysis. *Neurochem. Res.*, **20**, 1147–1153.

Costello, R.W., Fryer, A.D., Belmonte, K.E. & Jacoby, D.B. (1998) Effects of tachykinin KI1 receptor antagonists on vagal hyperactivity and neuronal M2 muscarinic receptor function in antigen challenged guinea pigs. *Br. J. Pharmacol.*, **124**, 267–276.

Deurveilher, S., Hars, B. & Hennevin, E. (1997) Pontine microinjection of carbachol does not reliably enhance paradoxical sleep in rats. *Sleep*, **20**, 593–607.

Drucker-Colín, R., Bernal-Pedraza, J., Fernández-Cancino, F. & Oksenberg, A. (1984) Is vasoactive intestinal polypeptide (VIP) a sleep factor? *Peptides*, **5**, 837–840.

Duffy, M., J. & Powell, D. (1975) Stimulation of brain adenylate cyclase activity by the undecapeptide substance P and its modulation by the calcium ion. *Biochem. Biophys. Acta.*, **385**, 275–280.

El Mansari, M., Sakai, K. & Jouvet, M. (1989) Unitary characteristics of presumptive cholinergic tegmental neurons during the sleep-waking cycle in freely moving cats. *Exp. Brain. Res.*, **76**, 519.

Garzon, M., De Andrés, I. & Reinoso-Suárez, F. (1998) Sleep patterns after carbachol delivery in the ventral oral pontine tegmentum of the cat. *Neuroscience*, **83**, 1137–1144.

Gerber, U., Stevens, D.R., McCarley, R.W. & Greene, R.W. (1991) Muscarinic agonists activate an inwardly rectifying potassium conductance in medial pontine reticular formation neurons of the rat in vitro. *J. Neurosci.*, **11**, 3861–3867.

Gnadt, J.W. & Pegram, G.V. (1986) Cholinergic brainstem mechanisms of REM sleep in the rat. *Brain Res.*, **384**, 29–41.

Greene, R.W., Gerber, U. & McCarley, R.W. (1989) Cholinergic activation of medial pontine reticular formation neurons *in vitro*. *Brain Res.*, **476**, 154–159.

Guevara Guzman, R., Kenrick, K.M. & Emson, P.C. (1993) Effect of

substance P on acetylcholine and dopamine release in the rat striatum: a microdialysis study. *Brain Res.*, **622**, 147–154.

Holzer, P. & Maggi, C.A. (1994) Synergistic role of muscarinic acetylcholine and tachykinin NK-2 receptors in intestinal peristalsis. *Naunyn. Schmiedebergs Arch. Pharmacol.*, **349**, 194–201.

Horstman, D.A., Takemura, H. & Putney, J.W. Jr (1988) Formation and metabolism of [^{3}H]inositol phosphates in AR42J pancreatoma cells. Substance P-induced Ca^{2+} mobilization in the apparent absence of inositol 1,4,5-trisphosphate 3-kinase activity. *J. Biol. Chem.*, **263**, 15297.

Inglis, W.L. & Semba, K. (1996) Colocalization of ionotropic glutamate receptor subunits with NADPH-diaphorase-containing neurons in the rat mesopontine tegmentum. *J. Comp. Neurol.*, **368**, 17–32.

Inoue, K., Nakazawa, K., Inoue, K. & Fujimori, K. (1995) Nonselective cation channels coupled with tachykinin receptors in rat sensory neurons. *J. Neurophysiol.*, **73**, 736–742.

Ito, K. & McCarley, R.W. (1984) Alterations in membrane potential and excitability of cat medial pontine reticular formation neurons during changes in naturally occurring sleep-wake states. *Brain Res.*, **292**, 169–175.

Jones, B.E. & Yang, T.-Z. (1985) The efferent projections from the reticular formation and the locus coeruleus studied by anterograde and retrograde axonal transport in the rat. *J. Comp. Neurol.*, **242**, 56–92.

Kamondi, A., Williams, J.A., Hutcheon, B. & Reiner, P.B. (1992) Membrane properties of mesopontine cholinergic neurons studied with the whole-cell patch-clamp technique: implications for behavioral state control. *J. Neurophysiol.*, **68**, 1359–1372.

Kayama, Y., Ohta, M. & Jodo, E. (1992) Firing of "possibly" cholinergic neurons in rat laterodorsal tegmental nucleus during sleep and wakefulness. *Brain Res.*, **569**, 210–220.

Kodama, T., Takahashi, Y. & Honda, Y. (1990) Enhancement of acetylcholine release during paradoxical sleep in the dorsal tegmental field of the cat brain stem. *Neurosci. Lett.*, **114**, 277–282.

Kohlmeier, K.A. & Reiner, P.B. (1999) Vasoactive intestinal polypeptide excites medial pontine reticular formation neurons in the brainstem rapid eye movement sleep-induction zone. *J. Neurosci.*, **19**, 4073–4081.

Koyano, K., Velimirovic, B.M., Grigg, J.J., Nakamjima, S. & Namajima, Y. (1993) Two signal transduction mechanisms of substance P-induced depolarization in locus coeruleus neurons. *Eur. J. Neurosci.*, **5**, 1189–1197.

Kungel, M., Ebert, U., Berbert, H. & Ostwald, J. (1994) Substance P and other putative transmitters modulate the activity of reticular pontine neurons: an electrophysiological and immunohistochemical study. *Brain Res.*, **643**, 29–39.

Leonard, T.O. & Lydic, R. (1997) Pontine nitric oxide modulates acetylcholine release, rapid eye movement sleep generation, and respiratory rate. *J. Neurosci.*, **17**, 774–785.

Lundberg, J.M. & Hökfeldt, T. (1983) Co-existence of peptides and classical neurotransmitters. *Trends Neurosci.*, **6**, 325–333.

Merritt, J.E. & Rink, T.J. (1987) The effects of substance P and carbachol on inositol tris-and tetrakisphosphate formation and cytosolic free calcium in rat parotid acinar cells. A correlation between inositol phosphate levels and calcium entry. *J. Biol. Chem.*, **262**, 14912.

Mistry, A. & Vijayan, E. (1987) Differential responses of hypothalamic cAMP and cGMP to substance P and neurotensin in ovariectomized rats. *Brain Res. Bull.*, **18**, 169–173.

Mitsuhashi, M., Ohashi, Y., Shichijo, S., Christian, C., Sudduth-Klinger, J., Harrowe, G. & Payan, D.G. (1992) Multiple intracellular signaling pathways of the neuropeptide substance P receptor. *J. Neurosci. Res.*, **32**, 437–443.

Morales, F.R., Xi, M.-C. & Chase, M.H. (1998) Induction of active sleep by atrial naturetic peptide microinjection within the nucleus pontis oralis of the cat. *Sleep Res.*, **21**, 33.

Moser, A. (1990) Guanine nucleotides regulate the effect of substance P on strital adenylate cyclase of the rat. *Biochem. Biophys. Res. Comm.*, **167**, 211–215.

Nakajima, Y., Tsuchida, K., Negishi, M., Ito, S. & Nakanishi, S. (1992) Direct linkage of three tachykinin receptors to stimulation of both phosphatidylinositol hydrolysis and cyclic AMP cascades in transfected chinese hamster ovary cells. *J. Biol. Chem.*, **267**, 2437–2442.

Nakaya, Y., Kaneko, T., Shigemoto, R., Nakanishi, S. & Mizuno, N. (1994) Immunohistochemical localization of substance P receptor in the central nervous system of the adult rat. *J. Comp. Neurol.*, **347**, 249–274.

Nelson, J.P., McCarley, R.W. & Hobson, J.A. (1983) REM sleep burst neurons, PGO waves and eye movement information. *J. Neurophysiol.*, **50**, 784–797.

Oakman, S.A., Faris, P.L., Cozzari, C. & Hartman, B.K. (1999) Characterization of the extent of pontomesencephalic cholinergic neurons' projections to the thalamus: Comparison with projections to midbrain dopaminergic groups. *Neuroscience*, **94**, 529–547.

Palkovits, M., Schmid, G., Bahner, U., Muller, I. & Heidland, A. (1990) Effects of centrally administered substance P on cyclic AMP levels in particular brain areas of rats. *Acta Morph. Hungarica*, **38**, 199–205.

Paxinos, G. & Watson, C. (1998). *The Rat Brain in Stereotaxic Coordinates*, 4th edn, Academic Press, New York.

Peralta, E.G., Ashkenazi, A., Winslow, J.W., Ramachandran, J. & Capon, D.J. (1988) Differential regulation of PI hydrolysis and adenylyl cyclase by muscarinic receptor subtypes. *Nature*, **334**, 434–437.

Reinoso-Suárez, F., De Andrés, I., Rodrigo-Angulo, M.L. & Rodriguez-Veiga, E. (1994) Location and anatomical connections of a paradoxical sleep induction site in the cat ventral pontine tegmentum. *Eur. J. Neurosci.*, **6**, 1829–1836.

Rye, D.B., Lee, H.J., Saper, C.B. & Wainer, B.H. (1988) Medullary and spinal efferents of the pedunculopontine tegmental nucleus and adjacent mesopontine tegmentum in the rat. *J. Comp. Neurol.*, **269**, 315–341.

Sakanaka, M., Shiosaka, S., Takatsuki, K., Inagaki, S., Takagi, H., Senba, E., Kawai, Y., Hara, Y., Iida, H., Minagawa, H., Matsuzaki, T. & Tohyama, M. (1981) Evidence for the existence of a substance P-containing pathway from the nucleus laterodorsalis tegmenti (Castaldi) to the lateral septal area of the rat. *Brain Res.*, **230**, 351–355.

Sakanaka, M., Shiosaka, S., Takatsuki, K. & Tohyama, M. (1983) Evidence for the existence of a substance P-containing pathway from the nucleus laterodorsalis tegmenti (Castaldi) to the medial frontal cortex of the rat. *Brain Res.*, **259**, 123–126.

Sastry, B.V. (1995) Neuropharmacology of nicotine: effects on the autoregulation of acetylcholine release by substance P and methionine enkephalin in rodent cerebral slices and toxicological implications. *Clin. Exp. Pharmacol. Physiol.*, **22**, 288–290.

Semba, K. (1993) Aminergic and cholinergic afferents to REM sleep induction regions of the pontine reticular formation in the rat. *J. Comp. Neurol.*, **330**, 543–556.

Semba, K. (1999) The mesopontine cholinergic system: A dual role in REM sleep and wakefulness. In Handbook of behavioral state control. In Lydic R. & Baghdoyan, H.A., (eds), *Cellular and Molecular Mechanisms*, pp. 161–180. CRC Press, Boca Raton.

Semba, K. & Fibiger, H.C. (1989) Organization of central cholinergic systems. *Prog. Brain Res.*, **79**, 37–63.

Semba, K., Reiner, P.B. & Fibiger, H.C. (1990) Single cholinergic mesopontine tegmental neurons project to both the pontine reticular formation and the thalamus in the rat. *Neuroscience*, **38**, 643–654.

Shammah-Lagnado, S.J., Negrão, N., Silva, B.A. & Ricardo, J.A. (1987) Afferent connections of the nuclei reticularis pontis oralis and caudalis: a horseradish peroxidase study in the rat. *Neuroscience*, **20**, 961–989.

Shen, K.Z. & North, R.A. (1992) Substance P opens cation channels and closes potassium channels in rat locus coeruleus neurons. *Neuroscience*, **50**, 345–353.

Stanfield, P.R., Nakajima, Y. & Yamaguchi, K. (1985) Substance P raises neuronal membrane excitability by reducing inward rectification. *Nature*, **315**, 498–501.

Steriade, M., Datta, S., Pare, D., Oakson, G. & Curró Dossi, R. (1990a) Neuronal activities in brain-stem cholinergic nuclei related to tonic activation processes in thalamocortical systems. *J. Neurosci.*, **10**, 2541–2559.

Steriade, M. & McCarley, R.W. (1990). *Brainstem Control of Wakefulness and Sleep*. Plenum Press, New York.

Steriade, M., Paré, D., Datta, S., Oakson, G. & Curró Dossi, R. (1990b) Different cellular types in mesopontine cholinergic nuclei related to ponto-geniculo-occipital waves. *J. Neurosci.*, **10**, 2560.

Sutin, E.L. & Jacobowitz, D.M. (1990) Localization of substance P mRNA in cholinergic cells of the rat laterodorsal tegmental nucleus: in situ hybridization histochemistry and immunocytochemistry. *Cell. Mol. Neurobiol.*, **10**, 19–31.

Valenta, D.C., Downing, J.E. & Role, L.W. (1993) Peptide modulation of ACh receptor desensitization controls neurotransmitter release from chicken sympathetic neurons. *J. Neurophysiol.*, **69**, 928–942.

Vanni-Mercier, G., Sakai, K. & Jouvet, M. (1989) Mapping of cholinoceptive brainstem structures responsible for the generation of paradoxical sleep in the cat. *Arch. Ital. Biol.*, **127**, 133–164.

Vertes, R.P. & Martin, G.F. (1988) Autoradiographic analysis of ascending projections from the pontine and mesencephalic reticular formation and the medial raphe nucleus in the rat. *J. Comp. Neurol.*, **275**, 511–541.

Vincent, S.R., Satoh, K., Armstrong, D.M. & Fibiger, H.C. (1983) Substance P in the ascending cholinergic reticular system. *Nature*, **306**, 688–691.

Wang, Y.-Y. & Aghajanian, G.K. (1987) Excitation of locus coeruleus neurons by an adenosine 3′5′-cyclic monophosphate-activated inward current. *Synapse*, **1**, 481–487.

Womack, M.D., Hanley, M.R. & Jessel, T.M. (1985) Functional substance P receptor on a rat pancreatic acinar cell line. *J. Neurosci.*, **12**, 3370.

Woolf, N.J. & Butcher, L.L. (1989) Cholinergic systems in the rat brain: IV. Descending projections of the pontomesencephalic tegmentum. *Brain Res. Bull.*, **23**, 519–540.

Yamamoto, K., Mamelak, A.N., Quattrochi, J.J. & Hobson, J.A. (1990) A cholinoceptive desynchronized sleep induction zone in the anterodorsal pontine tegmentum: Locus of the sensitive region. *Neuroscience*, **39**, 279–293.

Yoshimasa, T., Sibley, D.R., Bouvier, M., Lefkowitz, R.J. & Caron, M.G. (1987) Cross-talk between cellular signaling pathways suggested by phorbol-ester induced adenylate cyclase phosphorylation. *Nature*, **327**, 67–70.